İSTANBUL TEKNİK ÜNİVERSİTESİ ⋆ FEN BİLİMLERİ ENSTİTÜSÜ

MERKEZİ OLARAK ANKASTRE BİR DAİRESEL MEBRANIN DÜZLEMİNE DİK TİTREŞİM ANALİZİ

Yüksek Lisans Tezi
Barbaros SOYER , Müh.(İTÜ)

Ana Bilim Dalı : UÇAK MÜHENDİSLİĞİ
Programı : UÇAK MÜHENDİSLİĞİ

TEMMUZ 1992

ISTANBUL TECHNICAL UNIVERSITY ⋆ INSTITUTE OF SCIENCE AND TECHNOLOGY

ANALYSIS OF TRANSVERSE VIBRATIONS OF A CENTRALLY CLAMPED SPINNING MEMBRANE

M.Sc. THESIS
Barbaros SOYER , B.Sc.(ITU)

Date of Submission : June 22, 1992
Date of Approval : July 07, 1992

Supervisor : Assist.Prof.Dr. Temel KOTİL
Member : Assoc.Prof.Dr. Zahit MECİTOĞLU
Member : Assist.Prof.Dr. Hamza DİKEN

JULY 1992

ACKNOWLEDGEMENTS

I express sincere appreciation to Assistant Prof. Temel Kotil for his guidance and suggestions throughout this research, and also to the staff of the Education Center of the Istanbul Branch of the Chamber of the Turkish Mechanical Engineers for providing computers and facilities.

I also wish to thank Mr. Aydın Mısırlıoğlu for his continued interest in this study.

CONTENTS

LIST OF SYMBOLS

a	:	hub radius
b	:	membrane radius
k	:	spring coefficient
m	:	disk material density
n	:	number of nodal circle
u	:	transverse displacement
ω	:	frequency of transverse vibration
r, θ, t	:	radial, angular, and time variables
Ω	:	frequency of rotation
ψ	:	stress function
σ_r, σ_θ	:	normal stresses in polar coordinates
ξ_i	:	number of nodal diameter
ν	:	poisson's ratio
$\eta, \dot{\eta}$	:	initial generalized displacement and velocity

SUMMARY

Let us consider a circular membrane extending over a domain D defined by $a < r < b$. It is uniform, homogeneous, isotropic and has an angular velocity Ω (Fig. 2.3). The membrane on elastic foundation which is homogeneous is taken to be rigidly clamped on a circle of radius a and free at the outer edge, $r = b$. By taking an infinitesimal element of the membrane, equilibrium equations and in-plane stresses are obtained. The resultant expressions are same as those which are used in the studies of Barasch-Chen and Eversman. Then the equation of motion is derived by taking again an infinitesimal element in rectangular coordinate, and the equation of motion is transfered from (x, y) set to (r, θ) set. So the governing partial differantial equation is reached. In order to solve the governing differantial equation, separation of variable is used. Finally we reach an eigenvalue problem. After a comparison function is selected, stiffness and mass matrices are constructed by means of Rayleigh-Ritz method, and the governing differantial equation is numerically solved. The results are presented by using graphics and shapes.

Later the membrane is considered to subject the harmonic excitation. It is analyzed in the condition that its boundary at $r = a$ is subjected to translational harmonic motion in the form of $A \sin wt$. The governing differantial equation is modified and numerically solved by modal analysis. Again the results are presented graphically.

Finally a different approach to the problem is made. In order to solve the problem without elastic foundation a finite element software package, called "Applied Structure", is used. The stress and strain distributions, and mode shapes are presented graphically.

In this study it is shown that the frequencies of a centrally clamped spinning membrane are affected from the angular velocity and the clamped radius seriously. Mode shapes obtaining in the second chapter are similar to those obtaining by using Applied Structure software. This justifies that the results are accurate enough.

Using both FTN77 and AutoLISP programming languages, the vibration phenomena is succesfully simulated in this thesis.

ÖZET

MERKEZİ OLARAK ANKASTRE BİR DAİRESEL MEBRANIN DÜZLEMİNE DİK TİTREŞİM ANALİZİ

Dairesel diskler, bir çok kullanım alanının olmasından dolayı , eskiden olduğu gibi bugün de değişik mühendislik disiplinlerinin ilgisini çekmektedir. Farklı yükler altında, değişik sınır şartlarında dairesel diskler pratikte oldukça fazla uygulama alanı bulmaktadır. Solar yelkenler veya uzay araçları için optik veya radar yansıtıcılar, oldukça büyük ve eksenleri etrafında dönen dairesel diskler için iyi bir uygulama alanıdır. Son yıllarda modern bilgisayarlarda kayıt cihazı olarak kullanılan diskler (floppy disks) üzerindeki çalışmalar, ekseni etrafında dönen dairesel diskler için yeni bir uygulama alanı açmıştır. Bu geniş uygulama alanı dairesel diskler üzerindeki araştırmaların artacağını göstermektedir.

Dairesel disklerin analizi, stabilite, titreşim, gerilme dağılımı, tasarım, optimizasyon ve yer değiştirme konularında, çok fazla teorik ve deneysel çalışmayı içermektedir. Bu konularla ilgili problemlerin çözümünde genellikle sayısal çözüm metodlarına gereksinim duyulur. Çünkü analitik çözümler sadece dairesel disklerin özel durumları için vardır. Bunun sebebi, fiziksel olayı temsil eden diferansiyel denklemlerin karmaşıklığının ilave terimlerle hızla artmasıdır.

Bu çalışmada elastik homojen bir zemine oturan, düzlem, dairesel, homojen, izotropik ve çok ince bir diskin dinamik analizi üzerinde çalışılmıştır. Disk b yarıçapında olup, $r = a$ eğrisi boyunca ankastredir ve simetri ekseni etrafında Ω açısal hızı ile dönmektedir (Şekil 2.3).

İlk olarak, yukarıda geometrisi açıklanan disk üzerinden sonsuz küçük bir parça alınarak, bu eleman üzerine etkiyen kuvvetler düşünülmüş ve problemin tabiatından kaynaklanan eksenel simetri ve düzlem gerilme hali de göz önünde bulundurularak radyal ve açısal doğrultulardaki denge denklemleri

$$\frac{\partial \sigma_r}{\partial r} + \frac{\sigma_r - \sigma_\theta}{r} + m\Omega^2 r^2 = 0$$

$$\frac{1}{r}\frac{\partial \sigma_\theta}{\partial \theta} = 0$$

ve düzlem gerilmeler

$$\sigma_r = \frac{\mu_2}{r^2}(b^2 - r^2)\left\{r^2 + \frac{\mu_1}{b^2\mu_2}\right\}$$

$$\sigma_\theta = \frac{\mu_2}{r^2}\left\{(b^2 - \frac{\mu_1}{b^2\mu_2})r^2 - \frac{\mu_1}{\mu_2} - \frac{\mu_3}{\mu_2}r^4\right\}$$

formunda bulundu. μ_1, μ_2 ve μ_3 diskin iç yarıçapı a, dış yarıçapı b ve Poisson oranına bağlıdır.

$$\mu_1 = \frac{(1-\nu)m\Omega^2 a^2 b^2}{8} \frac{(3+\nu)b^2 - (1+\nu)a^2}{(1+\nu)b^2 + (1-\nu)a^2}$$

$$\mu_2 = \frac{3+\nu}{8} m\Omega^2$$

$$\mu_3 = \frac{1+3\nu}{8} m\Omega^2$$

Problemi temsil edecek olan hareket denklemini elde edebilmek için ilk olarak bazı kabullerde bulunulmuştur.

1. Disk yeterince incedir. Yani mükemmel derecede esnek ve eğilme momenti taşımamaktadır.
2. Disk üzerine etkiyen gerilme, sınıra normaldir.
3. Ağırlık kuvvetleri ihmal edilmiştir.
4. Disk düzleminden dışarı olan yer değiştirmeler diskin boyutlarına kıyasla çok küçüktür.
5. Eğim, bir birim yanında, oldukça küçüktür.
6. Düzlem yer değiştirmeler ihmal edilebilir mertebededir.

Yukarıdaki kabuller ışığında hareket denklemini elde edebilmek için, tekrar kartezyen koordinatlarda sonsuz küçük bir eleman alınıp, üzerine etkiyen kuvvetlere dikkat edilerek, z yönünde Newton'un ikinci kanununu tatbik etmek suretiyle, hareket denklemi kartezyen koordinatlarda türetilmiş olur. Anolojiden yararlanarak, bu hareket denklemi polar koordinatlara dönüştürülmüştür.

$$\frac{1}{r}\frac{\partial}{\partial r}(rdr\frac{\partial u}{\partial r}) + \frac{1}{r^2}\frac{\partial}{\partial \theta}(\sigma_\theta \frac{\partial u}{\partial \theta}) - ku - m\frac{\partial^2 u}{\partial t^2} = 0$$

Problemimizi temsil eden diferansiyel denkleme ulaştıktan sonra sınır şartları da aşağıdaki gibi alınabilir.

$$u(a,\theta,t) = 0$$

$$\frac{\partial^2 u(b,\theta,t)}{\partial r^2} = 0$$

$$u(r,\theta,t) = u(r,\theta+\pi,t)$$

$$\left(\frac{\partial u(r,\theta,t)}{\partial \theta}\right)_{\theta=\theta_0} = \left(\frac{\partial u(r,\theta,t)}{\partial \theta}\right)_{\theta=\theta_0+\pi}$$

Diferansiyel denklemi çözebilmek için aşağıdaki gibi bir değişken dönüşümü uygulanmıştır.

$$u(r,\theta,t) = W(r)\Theta(\theta)T(t)$$

Bir takım matematiksel işlemlerden sonra

$$T(t) = \cos(\omega t - \phi)$$

$$\Theta(\theta) = \cos(\xi_i \theta), \qquad \xi_i = 1, 2, \cdots$$

olarak bulunmuştur.

$W(r)$ fonksiyonunu bulabilmek için diğer iki çözümden yararlanıldığında, bir özdeğer problemi ile karşılaşılmaktadır. Bilindiği gibi özdeğer problemlerinin genel formu $L[W] = \lambda M[W]$ şeklindedir. Elimizdeki problem için L ve M operatörleri

$$L = \frac{1}{m}\frac{d}{dr}(r\sigma_r \frac{d}{dr}) - \xi_i^2 \frac{\sigma_\theta}{rm} - \frac{kr}{m}$$

$$M = -r$$

Bu aşamada Rayleigh-Ritz Metodu devreye sokularak, özdeğerler ve özvektörler, rijitlik ve kütle matrisleri bulunduktan sonra, elde edilmektedir. Bu değerler, daha önceden kabul ettiğimiz çözüm fonksiyonunda

$$W_n = \sum_{i=1}^{N} \alpha_i U_i(r)$$

yerine konarak $W(r)$ fonksiyonu bulunmuş oluyor. Yukarıda $W(r)$ için kabul edilen çözüm fonksiyonunda α_i 'ler özvektörler, $U_i(r)$ ise rastgele seçilen fakat bütün sınır şartlarını sağlayan bir karşılaştırma fonksiyonudur. Bizim uygulamalarımızda bu fonksiyon aşağıdaki gibi seçilmiştir.

$$U_i(r) = \sin\left[\frac{2\pi}{3} i \frac{(r-a)}{(b-a)}\right]$$

Görüldüğü gibi $u(r,\theta,t)$ fonksiyonu artık bilinmektedir. Sonuçta geometrimizin serbest titreşim analizi yapılmış ve titreşim modları grafik ve şekillerle sunulmuştur.

Daha sonra geometrimizin uyarılmaya karşı cevabı incelenmiştir. Disk $r = a$ eğrisi boyunca ankastreydi. Buradaki uyarılma, ankastrenin bilinen bir fonksiyon olan $u_0(t)$ miktarında z yönünde hareketidir. $u_0(t)$ rijit cisim hareketi ve $u(r,\theta,t)$, rijit cisim hareketine relatif olan elastik deformasyon olarak düşünüldüğünde, herhangi bir noktanın mutlak yer değiştirmesi

$$u_0(t) + u(r,\theta,t)$$

olarak alınabilir. Sistemimize etkiyen dış kuvvetler olmadığı için sistemimizi tarif eden diferansiyel denklem aşağıdaki gibidir.

$$L[u_0(t)+u(r,\theta,t)]+M(r,\theta)\frac{\partial^2}{\partial t^2}[u_0(t)+u(r,\theta,t)]=0$$

Gerekli matematik işlemlerden sonra denklemimiz

$$L[u(r,\theta,t)]+M(r,\theta)\frac{\partial^2 u(r,\theta,t)}{\partial t^2}=-M(r,\theta)\frac{\partial^2 u_0(t)}{\partial t^2}-A_l(r,\theta)u_0(t)$$

formunu alir. En son elde ettiğimiz denklemin sağ tarafının $f(r,\theta,t)$ gibi bir fonksiyon olduğu düşünülebilir. Bu durum bize, desteklerin hareketinden kaynaklanan titreşim probleminin, zorlanmiş titreşim problemi olarak çözüldüğünü gösteriyor. Sağdaki ifadenin ilk terimi yayılı atalet kuvvetini, ikinci terim ise elastik kuvvetleri temsil etmektedir. Bu çalışmada rijit cisim hareketini temsil eden $u_0(t)=A\sin wt$ olarak alınmıştır. Sistemimizin uyarılmaya karşı vermiş olduğu cevabı bulabilmek için elde edilen son haldeki diferansiyel denklem

$$L[u(r,\theta,t)]+M(r,\theta)\frac{\partial^2}{\partial t^2}[u(r,\theta,t)]=A(k-m\omega^2)\sin\omega t$$

Denklemin çözülebilmesi için bundan sonra yapılması gereken aşağıdaki gibi bir koordinat dönüşümü yapmaktır.

$$u(r,\theta,t)=\sum_{k=1}^{\infty}\kappa_k(r,\theta)\eta_k(t)$$

Bu dönüşümde kullanılan $\kappa_k(r,\theta)$ fonksiyonu önceden serbest titreşim analizi vasıtası ile hesaplanmıştı. Bu aşamada $\eta_k(t)$ fonksiyonunun model analizi vasıtası ile hesaplanması gerekmektedir. Bu fonksiyonu bulabilmek için kullanılan diferansiyel denklem

$$\ddot{\eta}_k(t)+\omega_k^2\eta_k(t)=N_k(t),\qquad k=1,2,\cdots$$

Burada

$$N_k(t)=\int_D \kappa_k(r,\theta)F(t)drd\theta$$

Laplace dönüşüm metodu kullanılarak

$$\eta_k(t)=\frac{1}{\omega_k}\int_0^t N_k(\tau)\sin\omega_k(t-\tau)d\tau+\eta_k(0)\cos\omega_r(t)+\dot{\eta}_k(0)\frac{\sin\omega_k t}{\omega_k},\qquad k=1,2,\cdots$$

formunda bulunur. Burada $\eta_k(0)$ ve $\dot{\eta}_k(0)$, başlangıçtaki genelleştirilmiş yer değiştirme ve hızdır ve aşağıdaki denklemler vasıtası ile bulunurlar.

$$\eta_r(0)=\int_D M(r,\theta)w_r(r,\theta)w(r,\theta,0)drd\theta$$

$$\dot{\eta}_r(0)=\int_D M(r,\theta)w_r(r,\theta)\dot{w}(r,\theta,0)drd\theta\quad r=1,2,3,\cdots$$

Fakat bizim problemimizdeki başlangıç koşulları

$$u(r,\theta,0) = 0$$

$$\dot{u}(r,\theta,0) = 0$$

olduğu için, genelleştirilmiş başlangıç koşulları da aşağıdaki gibidir.

$$\eta_k(0) = 0$$

$$\dot{\eta}_k(0) = 0$$

Sonuçta sistemimizin $r = a$ sınırının $u_0(t)$ fonksiyonu büyüklüğünce düzlemine dik istikamette (z yönünde) harekete maruz kalmasına (uyarılmasına) karşı gösterdiği cevabı sayısal olarak çözmüş oluyoruz. Modelimizin herhangi bir t anındaki deforme olmuş halini elde edebiliriz. Yine bu analiz ile ilgili sonuçlar şekiller halinde sunulmuştur.

Daha sonraki bölümde elimizdeki probleme değişik bir açıdan yaklaşılmıştır. Elastik zemin kaldırılmış ve problem "Applied Structure" adındaki bir yazılım içinde modellenmiştir. Bu analiz sonucunda disk üzerindeki gerilme dağılımları ve yer değişimleri üç boyutlu olarak renklendirilmiş şekilde elde edilmiştir. Fakat kullanılan bilgisayarın kapasitesinin yetersiz olmasından dolayı mod şekilleri ancak iki boyutlu olarak temsil edilebilmiştir.

Tezin sonucunda elde ettiğimiz grafikler gösteriyor ki; frekanslar, poisson oranından ve yay katsayısından yok denebilecek kadar az etkilenmektedir. Bunun yanında açısal hız ve mebranın iç yarıçapının değişimleri, frekansları oldukça etkilemektedir. Ayrıca, yapılan analiz sonucu bulunan mod şekilleri, Applied Structure yazılımının analizi sonucu bulunan mod şekilleri ile benzerlik göstermektedir.

CHAPTER 1

A REVIEW ON ANALYSIS OF CIRCULAR DISKS

1.1 Introduction

Circular membranes under different loads at different boundary conditions and different profiles have been a subject of interest of engineering. The possible use of large spinning membranes like disks as solar sails or optical and radar reflectors for space vehicles has led to a renewed interest in the problem of calculating the transverse vibrations of an elatic disk rotating at a constant speed. This subject traditionally has been studied in connection with gas and steam turbines. More recently the problem has arisen in the study of disks with much less stiffness such as the "floppy disk" recording devices of modern computers [1]. Application areas of circular membranes vary from machine parts to floppy disks. This widespread causes an increase of the study on disks.

Analysis of circular plates contains many theoretical and experimental studies on the stability, vibration, stress distribution, design, optimization, and deflection have long been an important problem in the literature on elasticity.

Solutions to the problems related to above often require numerical techniques. Analytical solution exists for only special class of circular disks due to

complexitity rapidly with additional terms.

1.2 The Former Studies

The earliest study of a vibrating, spinning, elastic disk appears to be that of Lamb and Southwell, who derived the respective contributions to the equations from bending stress and in-plane stress due to rotation. In that paper and a subsequent one by Southwell they examined the frequencies and and modes of free vibration for complete disks which were either very flexible or very stiff [1].

Simmonds [2] and Eversman [3] each studied the modes of free vibration in a centrally clamped spinning membrane for which bending stresses were ignored. Using numerical techniques they obtained plots of frequencies, for low-ordered modes, as a function of the clamp radius.

In Eversman and Dodson [4], a similar analysis of free vibration frequencies was performed, this time with bending stress retained in the problem. The problem treated in Ref.4, that of transverse vibrations of a spinning, centrally clamped circular disk, was contained in the class of problems treated by Mote [5]. In Ref.5 the approximate free vibration characteristics of centrally clamped, variable thickness disks were analyzed by the Rayleigh-Ritz technique. Natural frequencies of transverse vibration were computed, taking into consideration rotational and thermal in-plane stresses as well as purposely induced initial stresses. Ref.[5] indicates that initial stresses can significantly raise the minimum disk natural frequency throughout a prescribed rotational and thermal environment.

Haigh and Murdoch [6] presented a method of determinig the stress distribution in rotating axially symmetrical systems. The analysis was based on the three-dimensional equilibrium equations and was applicable to turbine wheels of

appreciable thichness for which the thin disk (plane-stress) theory gave only approximate results. Finally three-dimensional calculation results were compared with plane-stress theory results.

1.3 The Latter Studies

After 1970s researches on the circular disks have extended much more, especially on the subjects which are the optimization analysis, vibration, and stability.

Seireg and Surana [7] presented a prodecure for rational design of high speed rotating disks due to increasing emphasis on higher speeds and lower weights. In Ref.[7] optimum configurations were automatically calculated to satisfy the designers' objective within given constraints. [7] illustrated the applicability of programming techniques to the optimal selection of the dimensions for such disks.

In Ref.[8] two-dimensional and three–dimensional procedures for evaluation of stress distribution in rotating disks of nonuniform thickness with integral shafts were presented. The two-dimensional analysis was utilized in a design procedure to obtain the configuration of such disks. The three-dimensional analysis was then used for accurate evaluation of the stress distribution. A comparison between the results from the two and three-dimensional analyses was illustrated by several examples.

The equation of motion of a rotating disk, clamped at the inner radius and free at the outer radius, was solved by reducing the fourth-order equation of motion to a set of four first-order equations subject to arbitrary initial conditions (Barasch and Chen [9]). A modified Adam's method was used to numerically integrate the system of differential equations. Barasch and Chen showed that

Lamb-Southwell's approximate calculation of the frequency was justified.

In recent years the finite element method has been extensively developed, and has become established applications of the method to stress and vibration analysis of axisymmetric solids and disks given. In order to analyse the rotating disks under different loads at different boundary conditions, the finite element formulations started to be performed due to the developments in computer technology. Pardoen [10] discussed the static, vibration, and buckling analysis of axisymmetric circular plates using the finite element method. For the static analysis, the stiffness matrix of a typical annular plate was derived from the given displacement function and the appropriate constitutive relations. The static, vibration, and buckling analysis of isotropic, circular and annular plates were presented. In addition, the static analysis of circular and annular plates having a polar orthotropic material was discussed. The basis for these analyses was the presentation of exact displacement functions for circular and annular plates of isotropic and polar orthotropic materials.

Kirkhope and Wilson [11] applied the finite element method to the stress and vibration analysis of thin rotating disks. By making use of the axisymmetric properties, annular finite elements were derived which describe the bending and stretching of such disks and were characterized by having only four degrees of freedom. These elements incorporated the desired number of diametral nodes in their dynamic deflection functions, and allowed for any specified thickness variation in the radial direction. The resulting mathematical model is thus particularly efficient for numerical computation. The accuracy and convergence of the method was demonstrated by numerical comparison with both exact and experimental data.

In Ref. [12] Night and Olson presented a finite element formulation for the analysis of rotating disks in either a body-fixed or a space-fixed coordinate

system. The in-plane stress distribution resulting from the in-plane body force due to rotation was determined first by a plane stress finite element analysis. The resulting plane stresses were used as input to the out-of-plane or bending analysis. Additionally a direct method of determining the critical speeds through an eigenvalue analysis in space-fixed coordinates was presented. Then the undamped steady state response to a space-fixed transverse point load was examined. The effects of a viscous type damping were also presented.

Good and Lowery [13] constructed a finite element modeling of the free vibration of a read/write head floppy disk system. The objective of that work was to determine the design parameters of read/write head support structure which reduce the vibration phenomena.

Mote and Szymani [14] prepared a review report on principal developments in thin circular saw vibration and control research. That work was divided into two parts. The first part reviewed the general research results on saw vibration, saw stability, the critical speed theory and membrane stress effects on stability (tension, rotation and thermal effects). The influence of saw design and process parameters and aerodynamic loading on vibration were included. The second part concentrated on saw vibration reduction and control through saw design and membrane stress modification. Vibration noise control and feedback control of saw vibration and stability were also discussed.

Benson and Bogy [1] examined the problem of steady deflection of a very flexible spinning disk due to transverse loads that are fixed in space. They approached this problem within the context of membrane theory. The membrane differential operator was classified and shown to be hyperbolic in the outer region and elliptic in the inner portion. The eigenvalue problem was examined and the membrane operator was found to be singular. They therefore concluded that the problem of interest could not be solved within the context of membrane

theory. Finally the problem was formulated with bending stiffness retained. The concentrated load problem was solved by use of a Fourier series expansion in the angular direction in conjunction with a numerical solution for the radial modes. Graphical results were presented for various values of the stiffness parameter and load location.

1.4 Some Remarks

The importance of circular disks is increasing due to wide-spread use in technology. Circular disk research usually contains vibration, stability, stress distribution, deflections, tensioning, and rotation analysis.

Vibratory motion which is caused by normal disturbances must be between certain limits due to the harmful to products. As you know, it reduces product accuracy, diminishes surface quality, reduces tool life and increases machine down-time. The concept of resonance is important in understanding circular disk vibrations. Resonance occurs when the driving forces are sinusoidal at the natural frequency of the disk. In this case large amplitude vibration occurs. Of course the amplitude is controlled by damping. In order to diminish the vibratory motion, either the vibration modes must be changed or the driving forces must be changed or both of them. These tecniques are employed in the industry.

Rotating disks always vibrate. But they are not always unstable. One of the instability mechanisms is the critical speed instability that always takes place before buckling. Therefore it is more significant concept.

Additionally tensioning increases the critical speed at least 30 percent. It occurs by local plastic deformation or local heating.

The angular velocity induces only tensile membrane stresses. Natural

frequencies increase with rotation speed. Rotation causes instability due to the mechanism of moving load resonance and critical speed. The instability is not caused by the centrifugal forces. While the rotational forces are zero, if the plate is stationary and the forces affected as circumferential, the critical speed still exists.

In the stress analysis two-dimensional analysis and three-dimensional case are being used.But the accuracy of two-dimensional analysis is adequate. In addition, it is convenient for the computer time requirements which is very important in optimization process. Usually in the design and optimization problems two-dimensional analysis is more adequate but in stress analysis three-dimensional case is taken into consideration due to more accurate results.

CHAPTER 2

FORMULATION AND ANALYSIS

2.1 General Equations In Cylindrical Coordinates

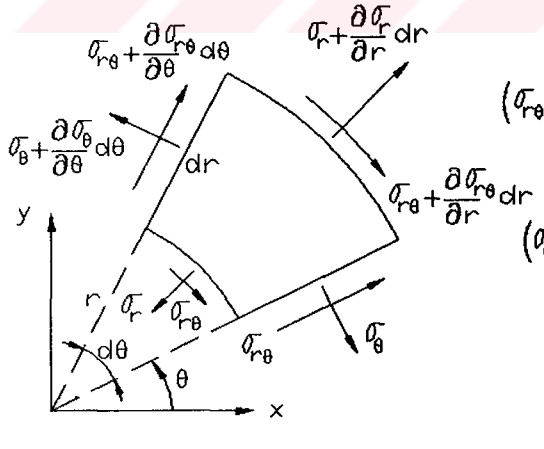

Figure 2.1 : Stresses on an infinitesimal element.

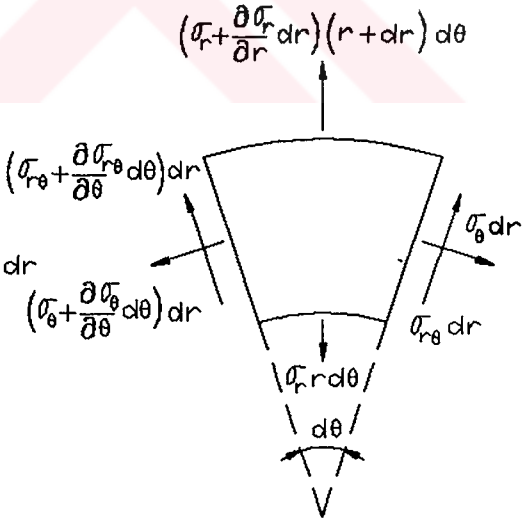

Figure 2.2 : Forces due to stresses.

Figure 2.1 shows stresses on an infinitesimal element of a thin circular disk. Figure 2.2 represents forces due to stresses acting on the element.

2.1.1 Equilibrium Equations And In–plane Stresses

F_r and F_θ are the body forces in r and θ directions. In the case of plane stress and plain strain $\sigma_{rz} = \sigma_{\theta z} = 0$. If we write equilibrium equations in the direction r by assuming that $d\theta/2$ is very small and neglecting higher order terms we get

$$\frac{\partial \sigma_r}{\partial r} dr r d\theta + \sigma_r dr d\theta - \sigma_\theta dr d\theta + \frac{\partial \sigma_{r\theta}}{\partial \theta} d\theta dr + F_r = 0 \qquad (2.1)$$

If this expression is divided by the element area which is approximately equal to $r d\theta dr$

$$\frac{\partial \sigma_r}{\partial r} + \frac{\sigma_r - \sigma_\theta}{r} + \frac{1}{r}\frac{\partial \sigma_{r\theta}}{\partial \theta} + F_r = 0 \qquad (2.2.a)$$

Similarly for the tangential component

$$\frac{1}{r}\frac{\partial \sigma_\theta}{\partial \theta} + \frac{\partial \sigma_{r\theta}}{\partial r} + \frac{2\partial \sigma_{r\theta}}{r} + F_\theta = 0 \qquad (2.2.b)$$

If the body forces are neglected then if we define following stress function

$$r\sigma_r = \psi \qquad (2.3.a)$$

$$\sigma_\theta = \frac{d\psi}{dr} \qquad (2.3.b)$$

Here the problem is axissymmetric so nothing depends on θ. Recall that

$$\varepsilon_r = \frac{du}{dr} \qquad (2.4.a)$$

$$\varepsilon_\theta = \frac{u}{r} \qquad (2.4.b)$$

From equations (2.2.a) and (2.4) we get the following compatibility equation

$$r\frac{d\varepsilon_\theta}{dr} + \varepsilon_\theta - \varepsilon_r = 0 \qquad (2.5)$$

Recall that

$$\varepsilon_\theta = \frac{1}{E}(\sigma_\theta - \nu\sigma_r) \qquad (2.6.a)$$

$$\varepsilon_r = \frac{1}{E}(\sigma_r - \nu\sigma_\theta) \qquad (2.6.b)$$

From equations (2.5) and (2.6) we obtain the compatibility equations in terms of stresses as

$$r\frac{d\sigma_\theta}{dr} - r\nu\frac{d\sigma_r}{dr} + \sigma_\theta(1+\nu) - \sigma_r(1+\nu) = 0 \tag{2.7}$$

In our problem the stresses are produced by the centrifugal loading on the membrane alone. So $F_r = m\Omega^2 r$, $F_\theta = 0$ where Ω is angular velocity. Under these conditions equation (2.2) take the following form

$$\frac{\partial\sigma_r}{\partial r} + \frac{\sigma_r - \sigma_\theta}{r} + m\Omega^2 r^2 = 0 \tag{2.8.a}$$

$$\frac{1}{r}\frac{\partial\sigma_\theta}{\partial\theta} = 0 \tag{2.8.b}$$

Let us define the following stress function which satisfy the equations (2.8)

$$r\sigma_r = \psi \tag{2.9.a}$$

$$\sigma_\theta = \frac{d\psi}{dr} + m\Omega^2 r^2 \tag{2.9.b}$$

If we substitute the equations (2.9) into the compatibility equation (2.7) we get

$$\frac{d^2\psi}{dr^2} + \frac{1}{r}\frac{d\psi}{dr} - \frac{\psi}{r^2} + (3+\nu)m\Omega^2 r = 0 \tag{2.10}$$

Solving this equation the stress function is

$$\psi = -\frac{(3+\nu)}{8}m\Omega^2 r^3 + c_1\frac{r}{2} + \frac{c_2}{r} \tag{2.11}$$

Inserting the solution to the equations (2.9) stresses are found with two unknowns which are integration constants.

$$\sigma_r = -\frac{(3+\nu)}{8}m\Omega^2 r^2 + \frac{c_1}{2} + \frac{c_2}{r^2} \tag{2.12.a}$$

$$\sigma_\theta = -\frac{3\nu+1}{8}m\Omega^2 r^2 + \frac{c_1}{2} - \frac{c_2}{r^2} \tag{2.12.b}$$

Integration constants can be determined by means of boundary conditions.The boundary conditions are

$$\sigma_r(b) = 0 \tag{2.13.a}$$

$$\varepsilon_\theta(a) = \frac{1}{E}(\sigma_\theta(a) - \nu\sigma_r(a)) = 0 \tag{2.13.b}$$

Applying the boundary conditions to the equations (2.12) and after some mathematical manipulations

$$\frac{c_1}{2} = m\Omega^2 b^2 \frac{(3+\nu)}{8} - \frac{(1-\nu)m\Omega^2 a^2}{8}\left\{\frac{(3+\nu)b^2-(1+\nu)a^2}{(1+\nu)b^2+(1-\nu)a^2}\right\} \qquad (2.14.a)$$

$$c_2 = \frac{(1-\nu)m\Omega^2 a^2 b^2}{8}\left\{\frac{(3+\nu)b^2-(1+\nu)a^2}{(1+\nu)b^2+(1-\nu)a^2}\right\} \qquad (2.14.b)$$

We can get σ_r and σ_θ by putting the equations (2.14) into the equations (2.12)

$$\sigma_r = \frac{\mu_2}{r^2}(b^2-r^2)\left\{r^2+\frac{\mu_1}{b^2\mu_2}\right\} \qquad (2.15.a)$$

$$\sigma_\theta = \frac{\mu_2}{r^2}\left\{(b^2-\frac{\mu_1}{b^2\mu_2})r^2-\frac{\mu_1}{\mu_2}-\frac{\mu_3}{\mu_2}r^4\right\} \qquad (2.15.b)$$

where

$$\mu_1 = \frac{(1-\nu)m\Omega^2 a^2 b^2}{8}\frac{(3+\nu)b^2-(1+\nu)a^2}{(1+\nu)b^2+(1-\nu)a^2}$$

$$\mu_2 = \frac{3+\nu}{8}m\Omega^2$$

$$\mu_3 = \frac{1+3\nu}{8}m\Omega^2$$

2.1.2 Vibration Of Circular Membrane

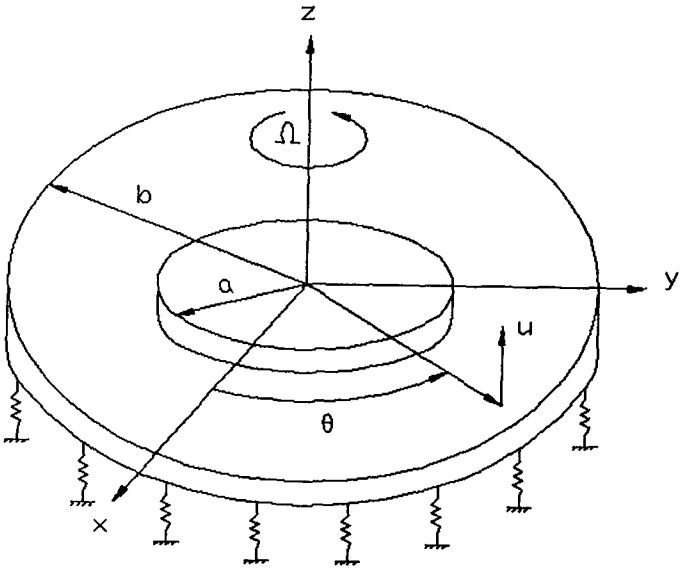

Figure 2.3 : Membrane geometry.

By referring to Figure 2.3, consider a uniform homogeneous isotropic circular membrane of radius b spinning about its polar axis with angular velocity Ω. The membrane on elastic foundation which is homogeneous is taken to be rigidly clamped on a circle of radius a, and free at the outer edge, $r = b$.

2.1.2.a Equation Of Motion

In order to reach equation of motion, firstly we can take an infinitesimal element in rectangular coordinate shown in Figures 2.4.

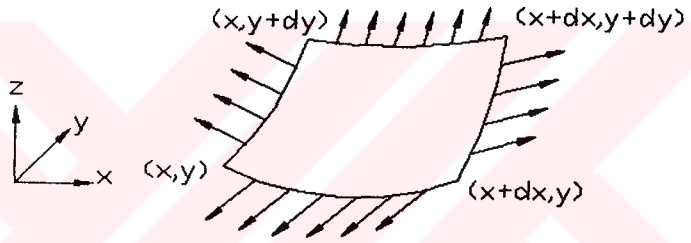

Figure 2.4.a : An infinitesimal element in rectangular element.

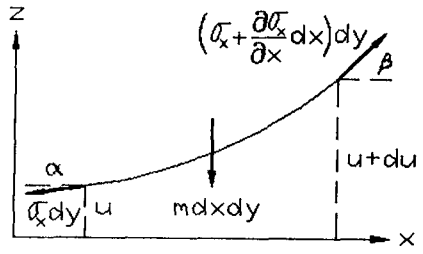

Figure 2.4.b : Projection in zx-plane.

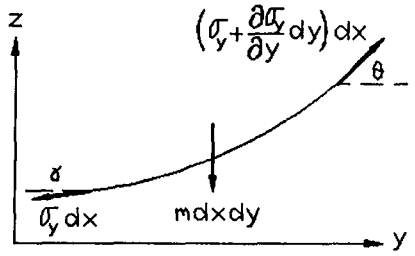

Figure 2.4.c : Projection in zy-plane.

The derivation of the equation of motion employs the following assumptions

1. The membrane is thin enough, that is, perfectly flexible, and cannot resist bending moment.

2. Tension acting on membrane is normal to boundary.
3. Gravity forces are neglected.
4. Transverse deflection is small with respect to dimensions of membrane.
5. Slop is small with respect to unity.
6. In-plane displacement is negligible.

From Figure 2.4.b and Figure 2.4.c slopes can be written as

$$\sin\alpha = \frac{\partial u}{\partial x} \tag{2.16.a}$$

$$\sin\beta = \frac{\partial u}{\partial x} + \frac{\partial}{\partial x}\left(\frac{\partial u}{\partial x}\right) dx \tag{2.16.b}$$

$$\sin\gamma = \frac{\partial u}{\partial y} \tag{2.16.c}$$

$$\sin\theta = \frac{\partial u}{\partial y} + \frac{\partial}{\partial y}\left(\frac{\partial u}{\partial y}\right) dy \tag{2.16.d}$$

Under these assumptions we can write the Newton's second law in direction z

$$\sum F_z = Ma_z$$

$$\begin{aligned} -\sigma_x dy\frac{\partial u}{\partial x} + (\sigma_x + \frac{\partial \sigma_x}{\partial x}dx)dy(\frac{\partial u}{\partial x} + \frac{\partial^2 u}{\partial x^2}dx) - \sigma_y dx\frac{\partial u}{\partial y} \\ +(\sigma_y + \frac{\partial \sigma_y}{\partial y}dy)dx(\frac{\partial u}{\partial y} + \frac{\partial^2 u}{\partial y^2}dy) - mgdxdy \;\; = \;\; mdxdy\frac{\partial^2 u}{\partial t^2} \end{aligned}$$

After some mathematical manipulations, and neglecting the high order terms , the equation of motion are obtained as

$$\sigma_x\frac{\partial^2 u}{\partial x^2} + \frac{\partial \sigma_x}{\partial x}\frac{\partial u}{\partial x} + \sigma_y\frac{\partial^2 u}{\partial y^2} + \frac{\partial \sigma_y}{\partial y}\frac{\partial u}{\partial y} = m\frac{\partial^2 u}{\partial t^2} \tag{2.17}$$

In analogy to go from (x, y) set to (r, θ) set

$$\frac{\partial}{\partial x} \longrightarrow \frac{\partial}{\partial r} \tag{2.18.a}$$

$$\frac{\partial^2}{\partial x^2} \longrightarrow \frac{\partial^2}{\partial r^2} \tag{2.18.b}$$

$$\frac{\partial}{\partial y} \longrightarrow \frac{1}{r}\frac{\partial}{\partial \theta} \tag{2.18.c}$$

$$\frac{\partial^2}{\partial y^2} \longrightarrow \frac{1}{r}\frac{\partial}{\partial r} + \frac{1}{r^2}\frac{\partial^2}{\partial \theta^2} \tag{2.18.d}$$

Applying the equations (2.18) into the equation (2.17), we obtain the equation of motion in circular coordinate.

$$\frac{1}{r}\frac{\partial}{\partial r}(rdr\frac{\partial u}{\partial r}) + \frac{1}{r^2}\frac{\partial}{\partial \theta}(\sigma_\theta \frac{\partial u}{\partial \theta}) = m\frac{\partial^2 u}{\partial t^2} \tag{2.19}$$

In order to take into consideration the effect of the elastic foundation in the equation (2.19) we have to insert an additional term. Therefore the equation (2.19) takes the following form

$$\frac{1}{r}\frac{\partial}{\partial r}(rdr\frac{\partial u}{\partial r}) + \frac{1}{r^2}\frac{\partial}{\partial \theta}(\sigma_\theta \frac{\partial u}{\partial \theta}) - ku - m\frac{\partial^2 u}{\partial t^2} = 0 \tag{2.20}$$

2.1.2.b Rayleigh-Ritz Method

Quite often it is sufficient to know the value of only a limited number of lowest frequencies rather than all the frequencies. The higher frequencies cannot be taken too seriously, even if an exact solution of the eigenvalue problem is obtained, because the assumptions employed in defining the models in most theories restricts the validity of the solutions to the lower modes only.

The method consists of selecting a trial family of compartison functions u_i ,satisfying all the boundary conditions, and constructing a linear combination

$$w_n = \sum_{i=1}^{n} a_i u_i$$

where the u_i are known functions, and the a_i are unknown coeffficients.

If we substitute w_n in Rayleigh's quotient we obtain

$$R(w_n) = \frac{\int_D w_n L[w_n] dD}{\int_D w_n M[w_n] dD} = \frac{N(w_n)}{D(w_n)}$$

Both the numerator and denominator depend on the function w_n and are both positive for a positive definite system.

The necessary conditions for the minimum of Rayleigh's quotient are

$$\frac{\partial R(w_n)}{\partial a_j} = \frac{D(w_n)\frac{\partial N(w_n)}{\partial a_j} - N(w_n)\frac{\partial D(w_n)}{\partial a_j}}{D^2(w_n)} = 0, \qquad j = 1, 2, \cdots, n$$

Recall that

$$\left[\frac{N(w_n)}{D(w_n)}\right]_{min} = \omega^2$$

Now introduce the notation

$$k_{ij} = \int_D u_i L[u_j] dD$$
$$m_{ij} = \int_D u_i M[u_j] dD \quad i, j = 1, 2, \cdots, n$$

and if the system is self- adjoint we have

$$k_{ij} = k_{ji} \qquad m_{ij} = m_{ji}$$

The operators L and M are linear, so we can write

$$N = \sum_{i=1}^{n}\sum_{j=1}^{n} k_{ij} a_i a_j$$

and, similarly

$$D = \sum_{i=1}^{n}\sum_{j=1}^{n} m_{ij} a_i a_j$$

Taking the partial derivatives with respect to a_r, we write

$$\frac{\partial N}{\partial a_r} = 2\sum_{j=1}^{n} k_{rj} a_j$$
$$\frac{\partial D}{\partial a_r} = 2\sum_{j=1}^{n} m_{rj} a_j \quad r = 1, 2, \cdots, n$$

Finally we obtain

$$\sum_{j=1}^{n} (k_{rj} - \omega_n^2 m_{rj}) a_j = 0, \qquad r = 1, 2, \cdots, n$$

which represents a set of n homogeneous algebraic equation in the unknowns a_j are known as Galerkin's equations. They represent the eigenvalue problem for an n-degree-of-freedom system and can be written in the matrix form

$$[k]\{a\} = \omega_n^2[m]\{a\}$$

where $[k]$ and $[m]$ are $n \times n$ symmetric matrices.

2.2 Solution Of The Governing Differantial Equation

In our problem, equation of motion is derived in the equation (2.20). Boundary conditions are

$$u(a,\theta,t) = 0 \tag{2.21.a}$$

$$\frac{\partial^2 u(b,\theta,t)}{\partial r^2} = 0 \tag{2.21.b}$$

$$u(r,\theta,t) = u(r,\theta+\pi,t) \tag{2.21.c}$$

$$\left(\frac{\partial u(r,\theta,t)}{\partial \theta}\right)_{\theta=\theta_0} = \left(\frac{\partial u(r,\theta,t)}{\partial \theta}\right)_{\theta=\theta_0+\pi} \tag{2.21.d}$$

2.2.1 Eigenvalue Problem

In order to solve the problem we can use separation of variables as

$$u(r,\theta,t) = W(r)\Theta(\theta)T(t) \tag{2.22}$$

After substitution the equation (2.22) into the equation (2.20) then division by $W(r)\Theta(\theta)T(t)$

$$\frac{1}{mWr}\frac{d}{dr}(r\sigma_r\frac{dW}{dr}) + \frac{1}{m\Theta r^2}\frac{d}{d\theta}(\sigma_\theta\frac{d\Theta}{d\theta}) - \frac{k}{m} = \frac{1}{T}\frac{d^2T}{dt^2} \tag{2.23}$$

Since right side is only function of t

$$\frac{1}{T}\frac{d^2T}{dt^2} = -\lambda \tag{2.24}$$

$$\frac{d^2T}{dt^2} + \lambda T = 0 \tag{2.25}$$

General solution of the equation (2.25) is

$$T(t) = \cos(\omega t - \phi) \tag{2.26}$$

The equation (2.23) becomes

$$\frac{1}{mWr}\frac{d}{dr}(r\sigma_r\frac{dW}{dr}) + \frac{1}{m\Theta r^2}\frac{d}{d\theta}(\sigma_\theta\frac{d\Theta}{d\theta}) - \frac{k}{m} = -\lambda \tag{2.27}$$

Multiply the equation (2.27) by mr^2 and rearranging

$$-\frac{r}{W\sigma_\theta}\frac{d}{dr}(r\sigma_r\frac{dW}{dr}) - \frac{r^2m\lambda}{\sigma_\theta} + \frac{kr^2}{\sigma_\theta} = \frac{1}{\Theta}\frac{d^2\Theta}{d\theta^2} \tag{2.28}$$

Since right side is only function of θ

$$\frac{1}{\Theta}\frac{d^2\Theta}{d\theta^2} = -\xi^2$$

$$\frac{d^2\Theta}{d\theta^2} + \xi^2\Theta = 0 \tag{2.30}$$

General solution of this equation is

$$\Theta(\theta) = A\cos(\xi\theta) + B\sin(\xi\theta) \tag{2.31}$$

From the equations (2.21.c) and (2.21.d)

$$\Theta(\theta) = \Theta(\theta + \pi) \tag{2.32}$$

$$\left(\frac{d\Theta}{d\theta}\right)_{\theta=\theta_0} = \left(\frac{d\Theta}{d\theta}\right)_{\theta=\theta_0+\pi} \tag{2.33}$$

Applying the boundary conditions (2.32) and (2.33) into the equation (2.31) to calculate the unknowns A and B we obtain

$$\Theta(\theta) = \cos(\xi_i\theta), \qquad \xi_i = 1, 2, \cdots \tag{2.34}$$

If the equation (2.29) is substituted into the equation (2.28)

$$-\frac{r}{W\sigma_\theta}\frac{d}{dr}(r\sigma_r\frac{dW}{dr}) - \frac{r^2m\lambda}{\sigma_\theta} + \frac{kr^2}{\sigma_\theta} = -\xi_i^2 \tag{2.35}$$

After some arrangement the equation becomes

$$\frac{1}{m}\frac{d}{dr}(r\sigma_r\frac{dW}{dr}) - \xi_i^2\frac{\sigma_\theta}{rm}W - \frac{kr}{m}W + \lambda rW = 0 \tag{2.36}$$

As it is seen, we reach an eigenvalue problem

2.2.2 Solution Of The Eigenvalue Problem

Consider the eigenvalue problem in the form

$$L[W] = \lambda M[W] \tag{2.37}$$

Here L and M operator are

$$L = \frac{1}{m}\frac{d}{dr}(r\sigma_r\frac{d}{dr}) - \xi_i^2\frac{\sigma_\theta}{rm} - \frac{kr}{m} \tag{2.38}$$

$$M = -r \tag{2.39}$$

Consider one of the solution of the equation (2.37) W_r and λ_r

$$L[W_r] = \lambda_r M[W_r] \tag{2.40}$$

In order to obtain Rayleigh's Quotient multiply the equation (2.40) by W_r and integrate over the domain and extract λ_r

$$\lambda_r = \frac{\int_D L[W_r]dD}{\int_D M[W_r]dD} \tag{2.41}$$

If we apply this procedure to our problem Rayleigh's Quotient is

$$R = \frac{\int_a^b \frac{1}{m}\frac{d}{dr}(r\sigma_r\frac{dW}{dr})W\,dr - \int_a^b \xi_i^2\frac{\sigma_\theta}{rm}W^2dr - \int_a^b \frac{kr}{m}W^2dr}{\int_a^b rW^2dr} \tag{2.42}$$

Take the first term in the numerator which needs some work and by using integration by parts

$$\int_a^b \frac{1}{m}r\sigma_r\frac{dW}{dr}\frac{dW}{dr}dr = \frac{1}{m}r\sigma_r\frac{dW}{dr}W|_a^b - \int_a^b \frac{1}{m}\frac{d}{dr}(r\sigma_r\frac{dW}{dr})W\,dr \tag{2.43}$$

Since $\sigma_r(b) = 0$ and $W(a) = 0$,

$$\frac{1}{m}r\sigma_r\frac{dW}{dr}W|_a^b = 0 \tag{2.44}$$

From the equation (2.44) Rayleigh's Quotient becomes

$$R = \frac{\frac{1}{m}\int_a^b r\sigma_r(\frac{dW}{dr})^2 + \int_a^b \xi_i^2\frac{\sigma_\theta}{rm}W^2dr + \int_a^b \frac{kr}{m}W^2dr}{\int_a^b rW^2dr} \tag{2.45}$$

Assume solution is

$$W_n = \sum_{i=1}^{N} \alpha_i U_i(r) \tag{2.46}$$

Applying Rayleigh's Ritz method, stiffness and mass matrices are

$$K_{ij} = \frac{1}{m}\int_a^b r\sigma_r \frac{dU_i(r)}{dr}\frac{dU_i(r)}{dr}dr + \int_a^b \xi^2 \frac{\sigma_\theta}{rm} U_i(r)U_j(r)dr +$$

$$\int_a^b \frac{kr}{m} U_i(r)U_j(r)dr \tag{2.47}$$

$$M_{ij} = \int_a^b rU_i(r)U_j(r)dr \tag{2.48}$$

Finally eigenvalue problem becomes

$$[[K_{ij}] - \lambda[M_{ij}]]\,[\alpha_i] = 0 \tag{2.49}$$

2.3 Numerical Results

In this analysis the following admissible function, an arbitrary function, satifying all boundary conditions, is used.

$$U_i(r) = \sin\left(\frac{2\pi}{3} i \frac{r-a}{b-a}\right)$$

In solution the first fourteen terms are taken into consideration. The results obtaining in this chapter are presented in the following pages by being used graphics and shapes.

The frequency is increasing with increasing the coefficient of the springs representing the elastic foundation, and the values of Poisson ratio so slowly that this effect on the frequencies can be neglected. But the effect of the angular velocity and the clamp radius on the frequencies is appearing obviously.

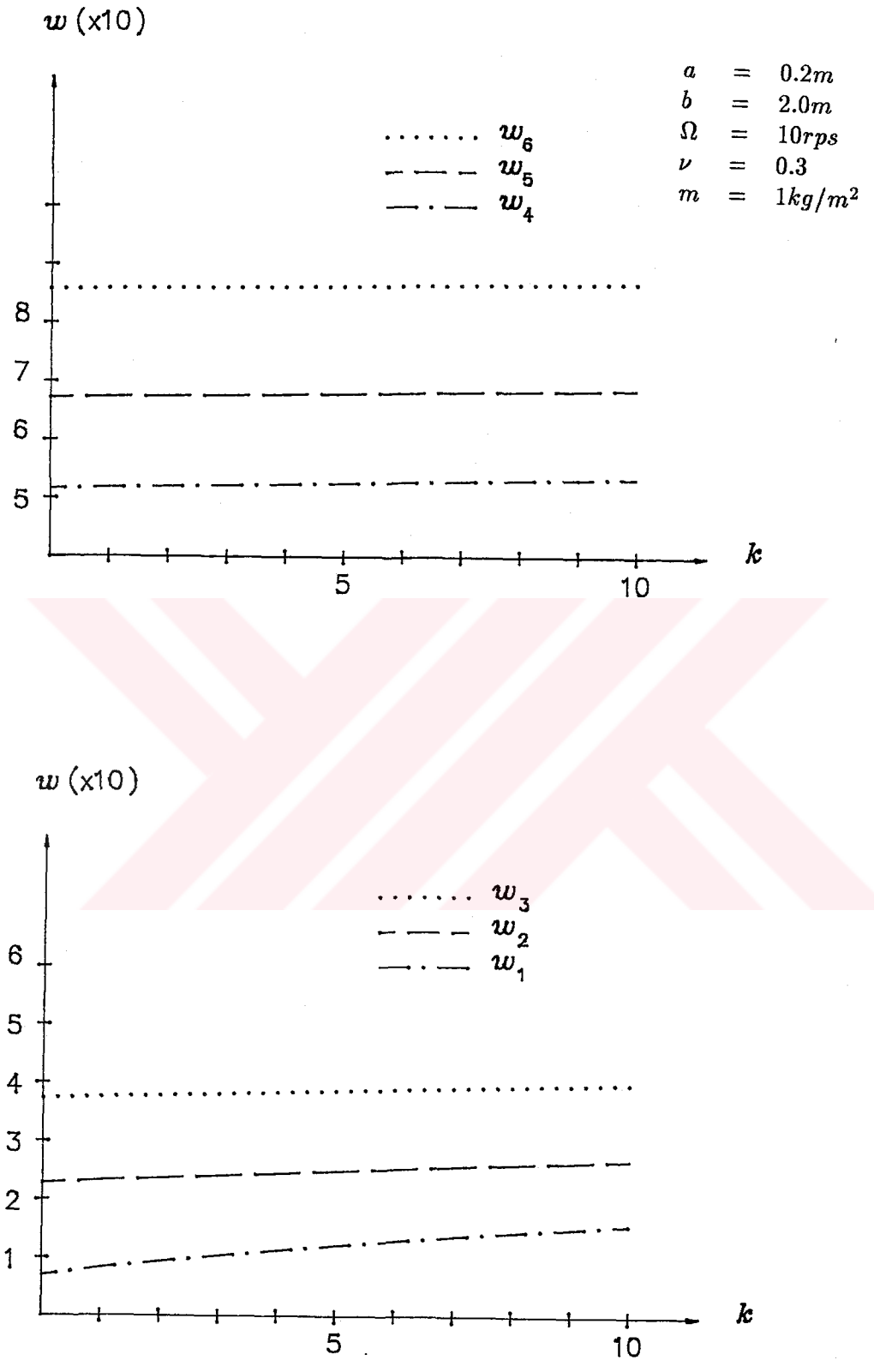

Figure 2.5 : Frequency versus the elastic foundation coefficient k. (0 nodal diameter.)

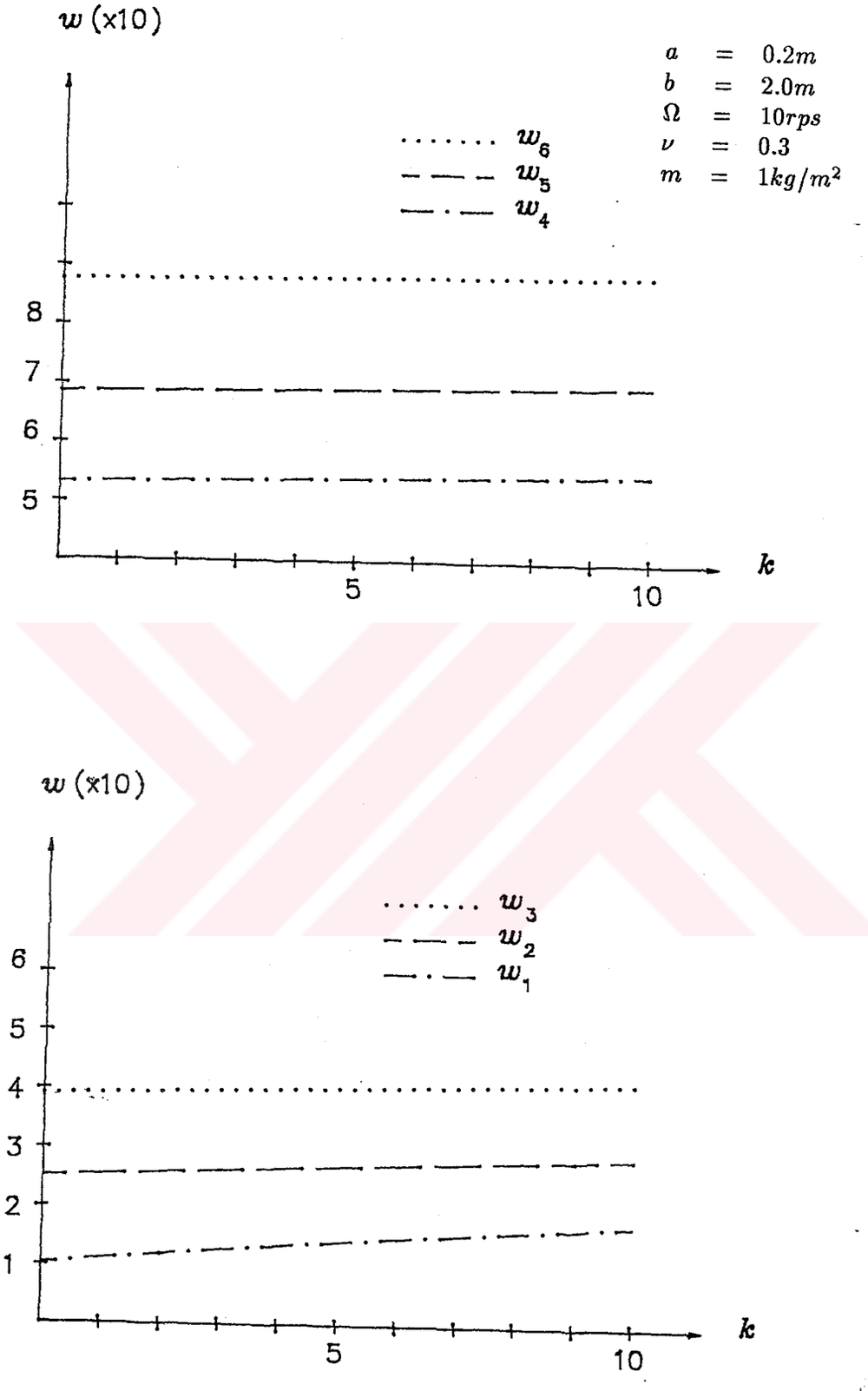

Figure 2.6 : Frequency versus the elastic foundation coefficient k. (1 nodal diameter.)

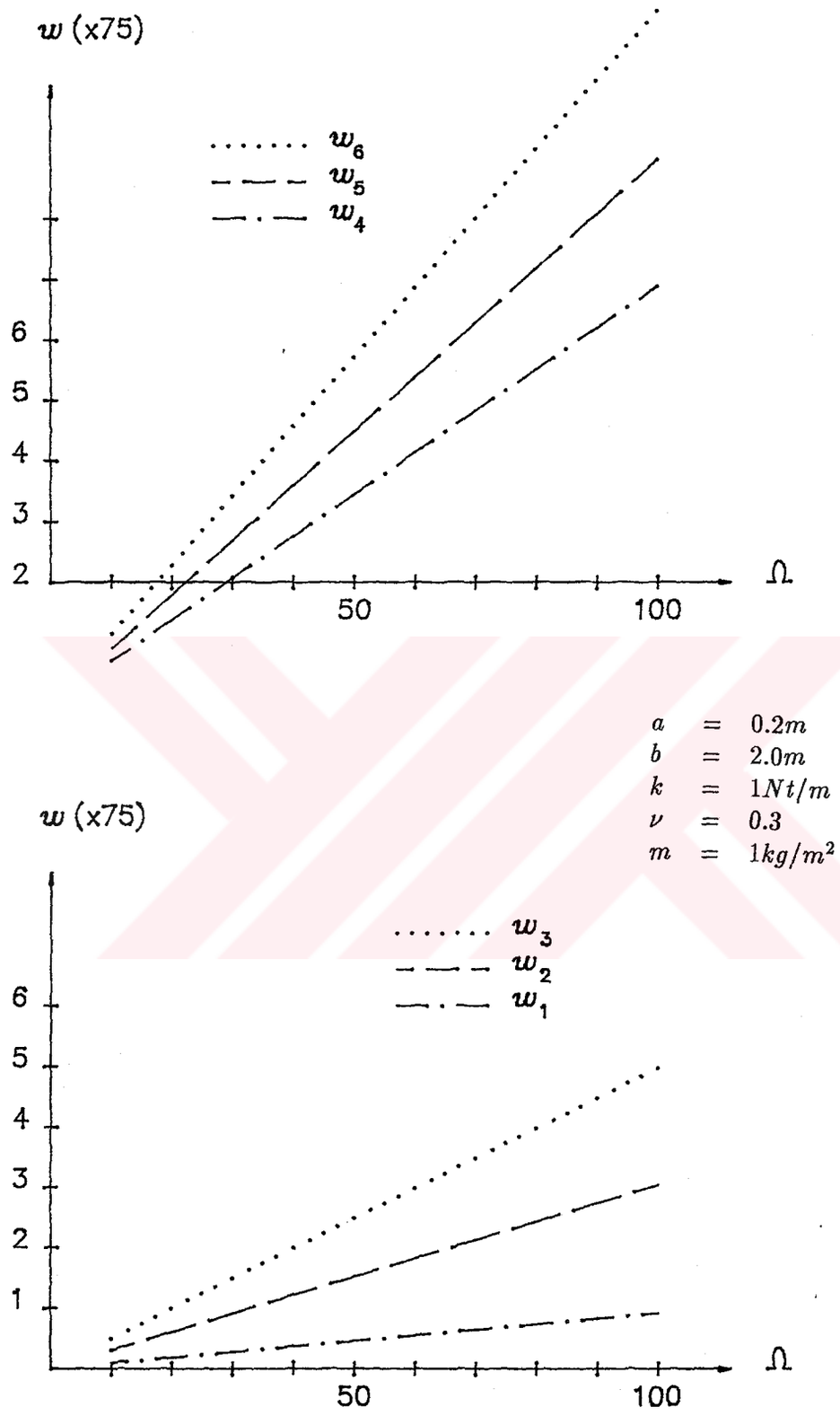

Figure 2.7 : Frequency versus the angular velocity Ω.
(0 nodal diameter.)

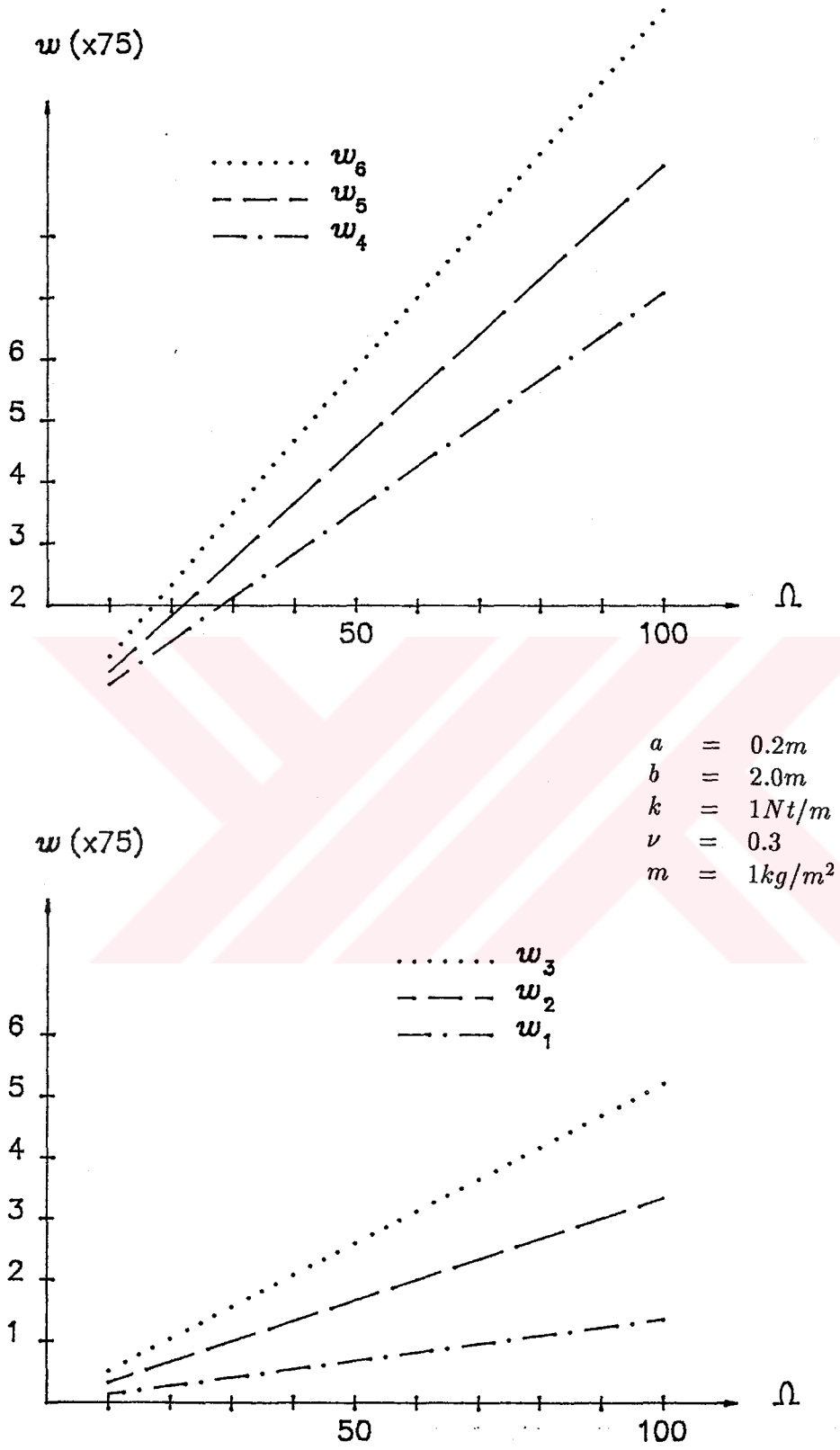

Figure 2.8 : Frequency versus the angular velocity Ω.
(1 nodal diameter.)

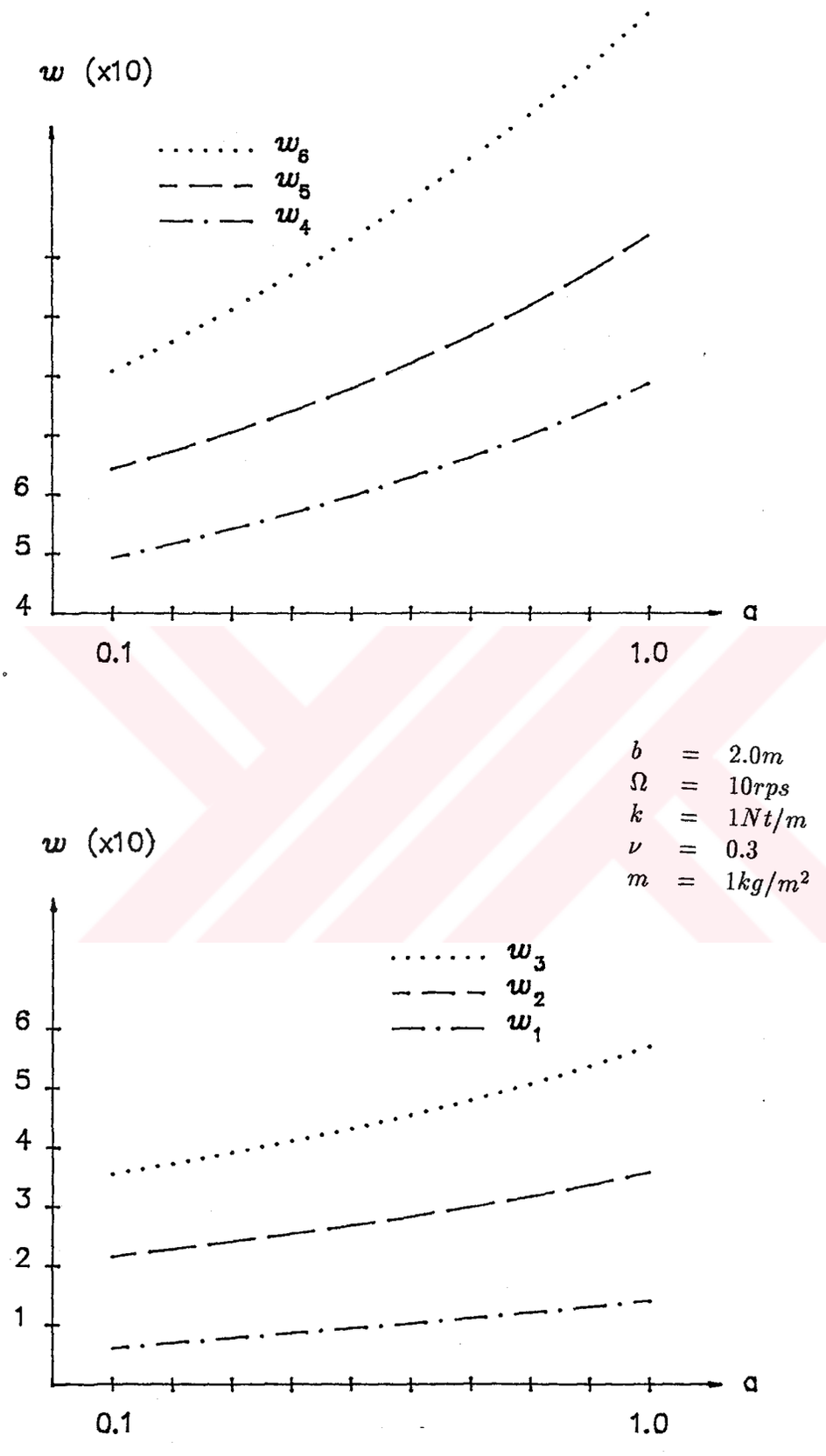

Figure 2.9 : Frequency versus the clamp radius a.
(0 nodal diameter.)

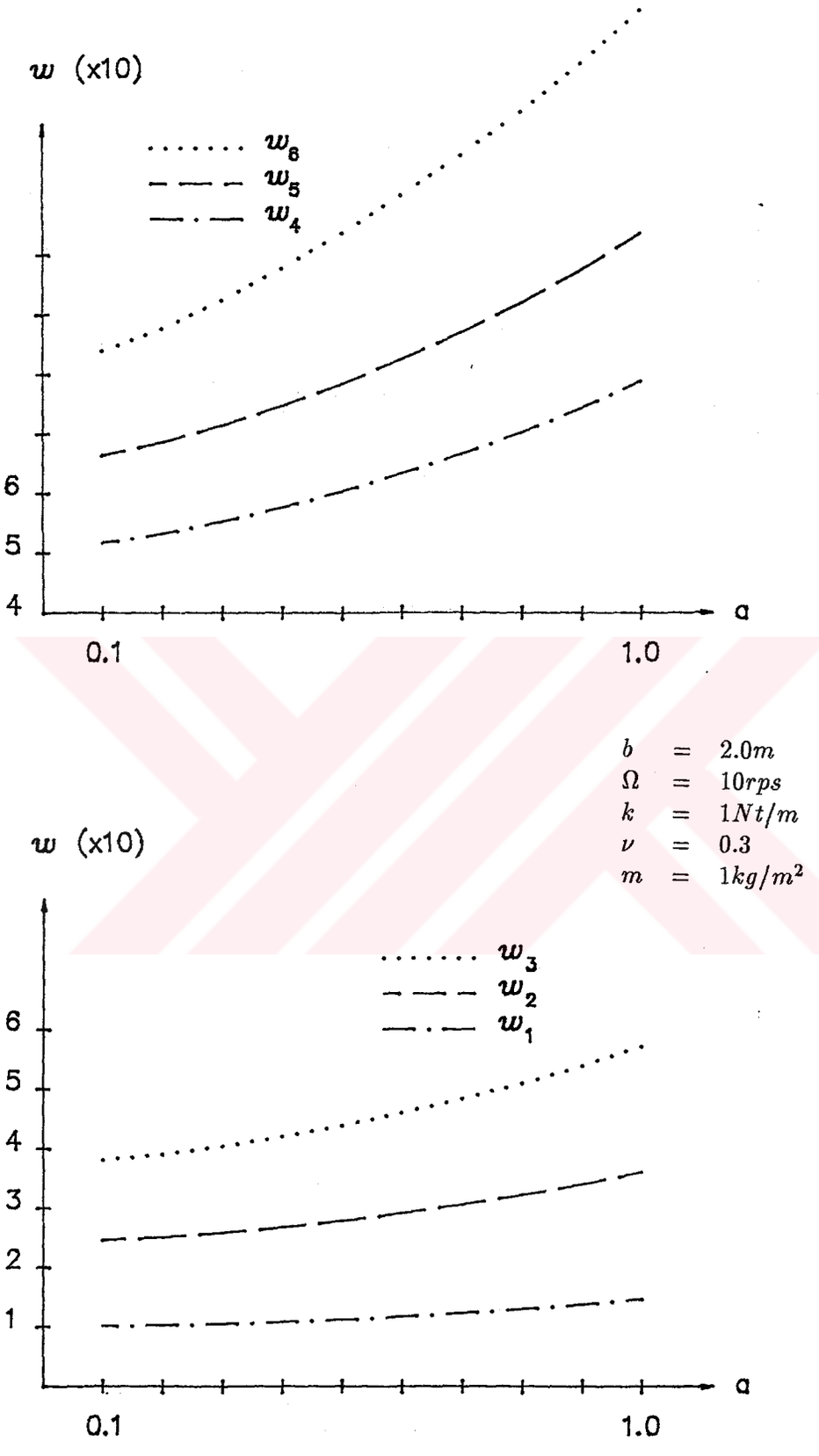

Figure 2.10 : Frequency versus the clamp radius a.
(1 nodal diameter.)

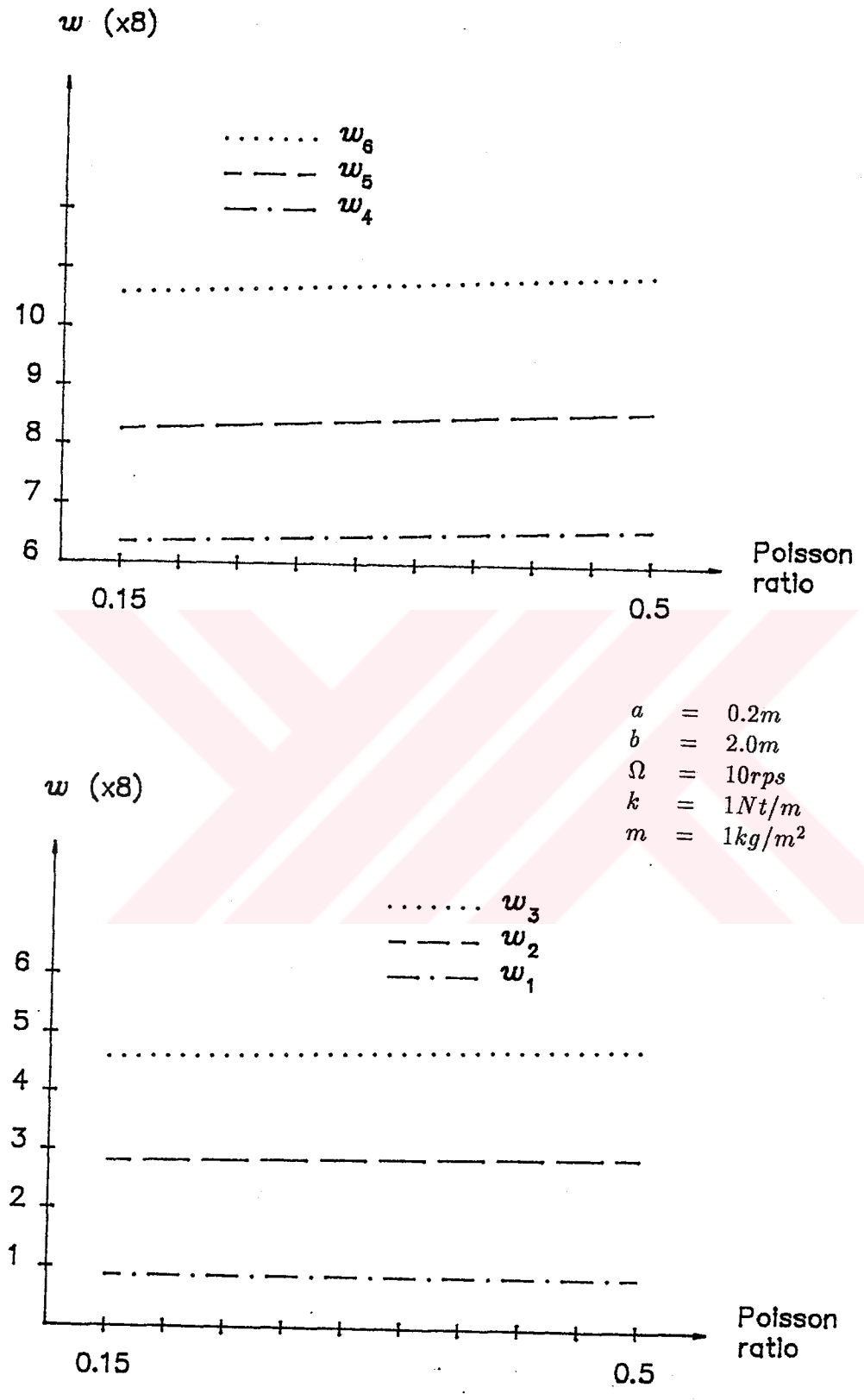

Figure 2.11 : Frequency versus Poisson ratio ν
(0 nodal diameter.)

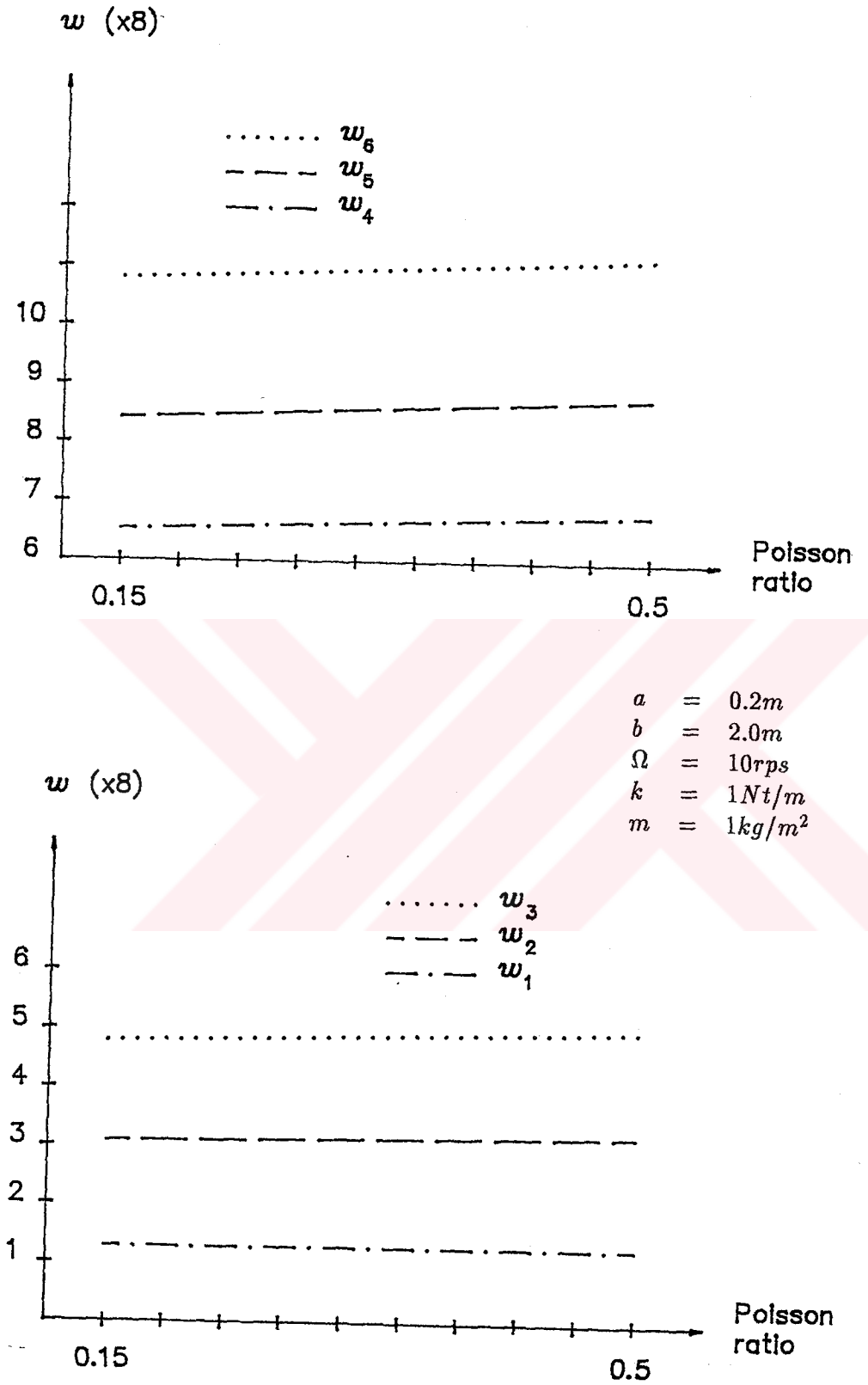

Figure 2.12 : Frequency versus Poisson ratio ν.
(1 nodal diameter.)

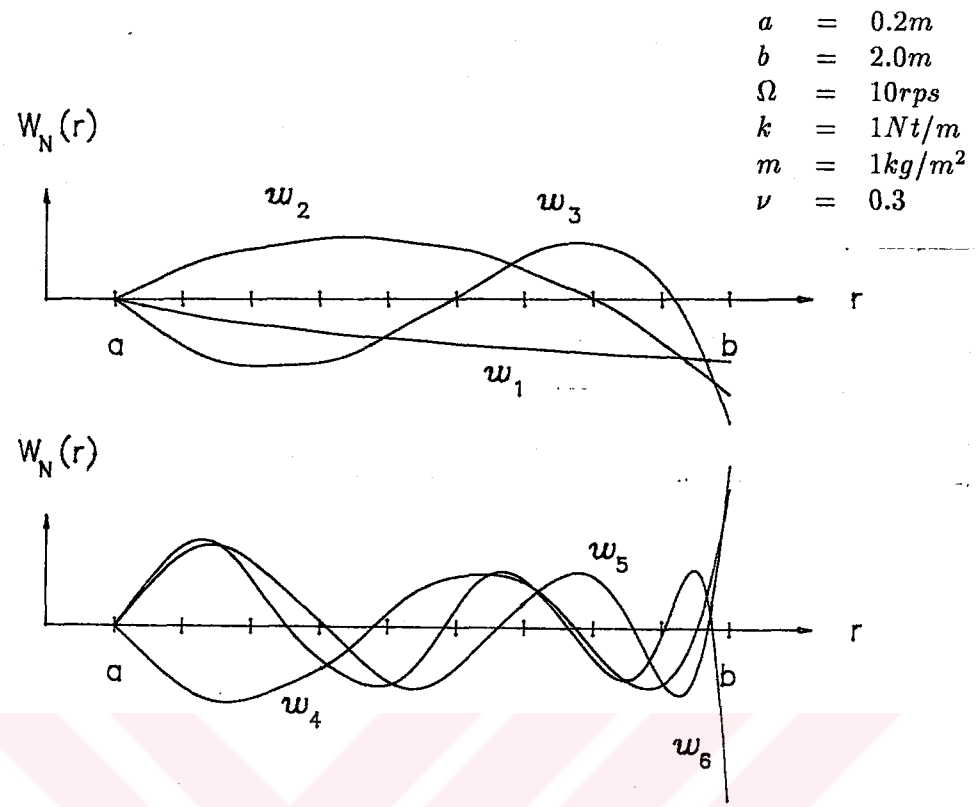

Figure 2.13 : 2-Dimensional mode shapes. (0 nodal diameter.)

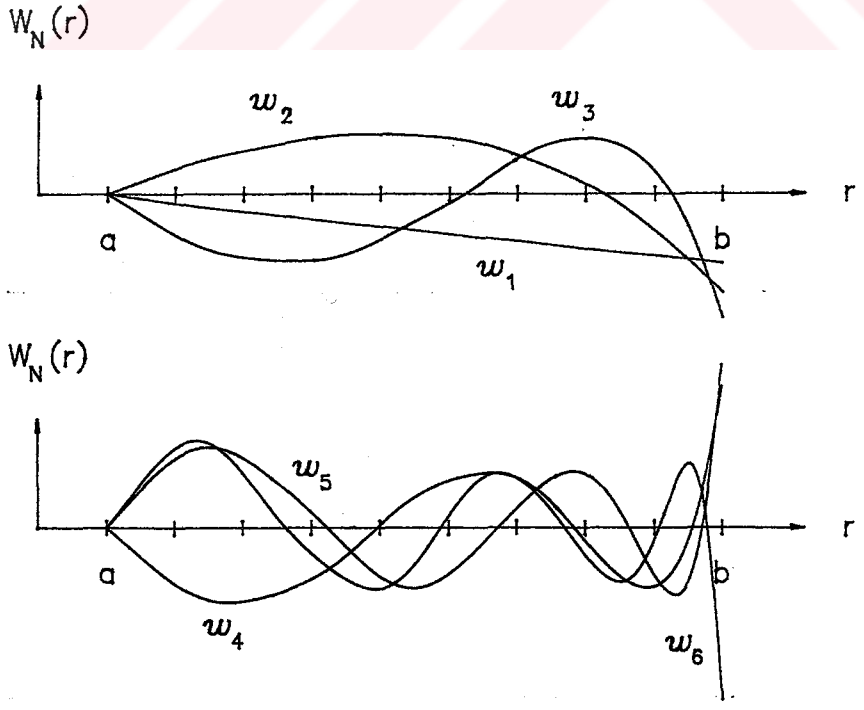

Figure 2.14 : 2-Dimensional mode shapes. (1 nodal diameter.)

$a = 0.2m$
$b = 2.0m$
$\Omega = 10rps$
$k = 1Nt/m$
$m = 1kg/m^2$
$\nu = 0.3$

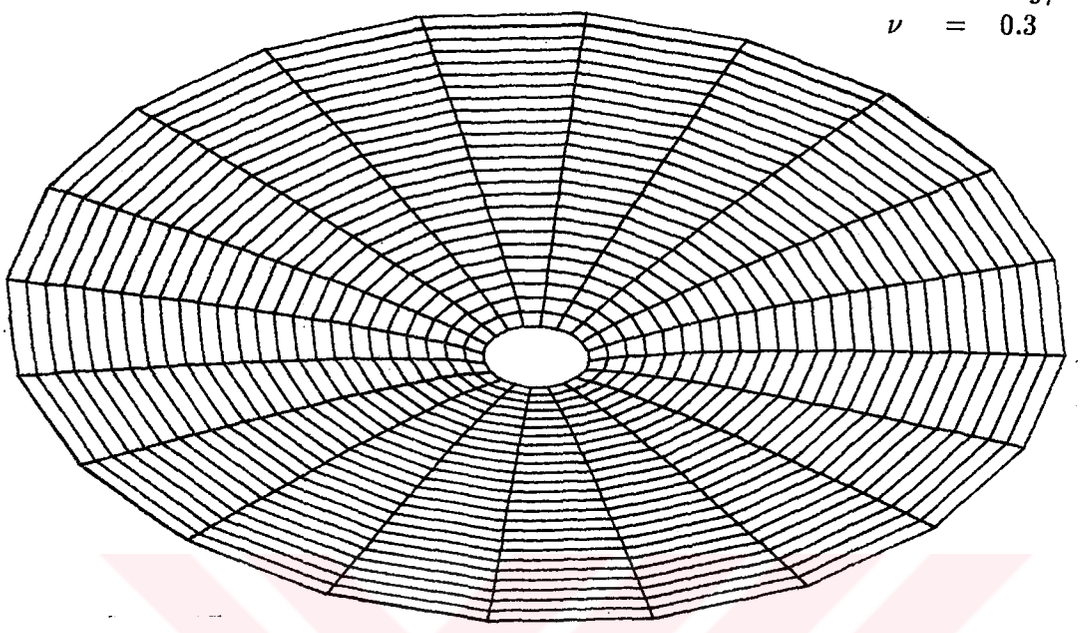

Figure 2.15 : Mode shape corresponding to 0 nodal diameter and 1 nodal circle

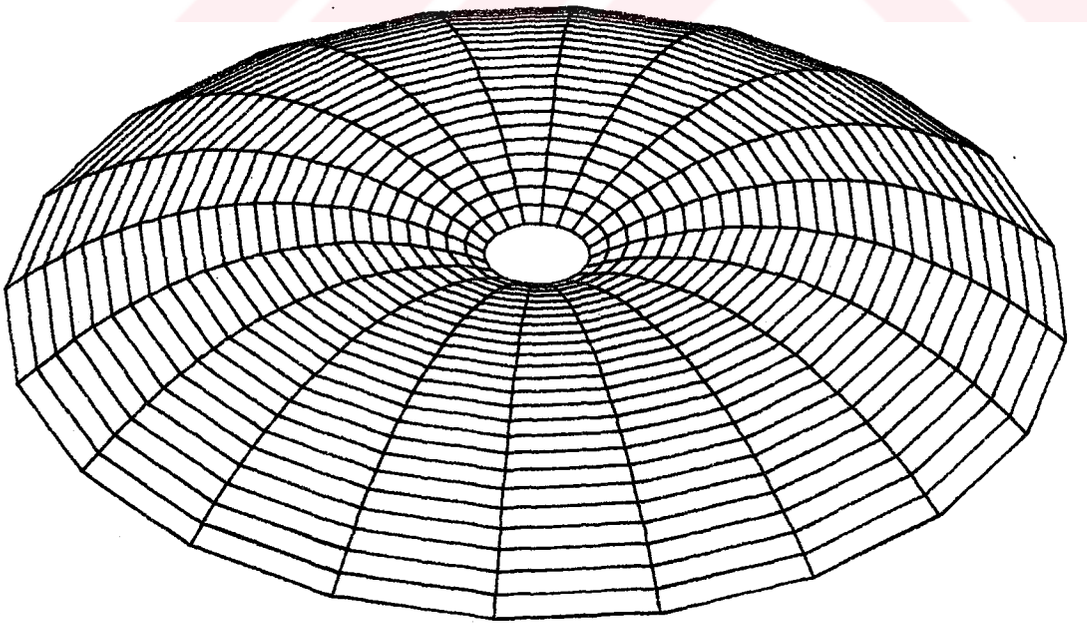

Figure 2.16 : Mode shape corresponding to 0 nodal diameter and 2 nodal circle

$a = 0.2m$
$b = 2.0m$
$\Omega = 10rps$
$k = 1Nt/m$
$m = 1kg/m^2$
$\nu = 0.3$

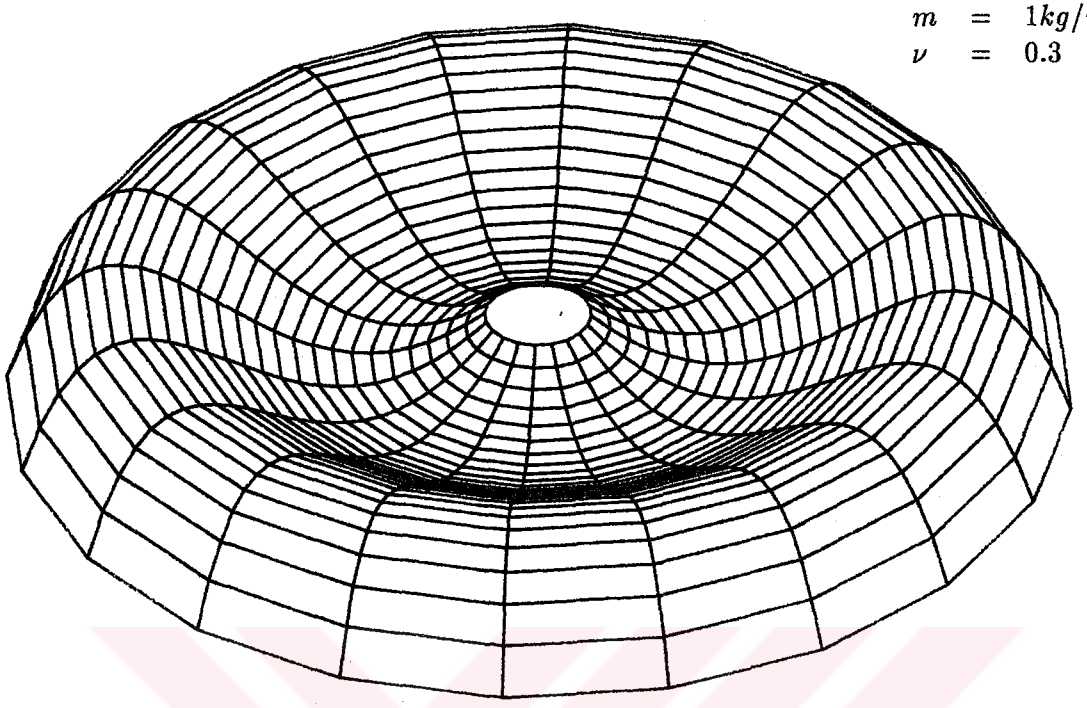

Figure 2.17 : Mode shape corresponding to 0 nodal diameter and 3 nodal circle

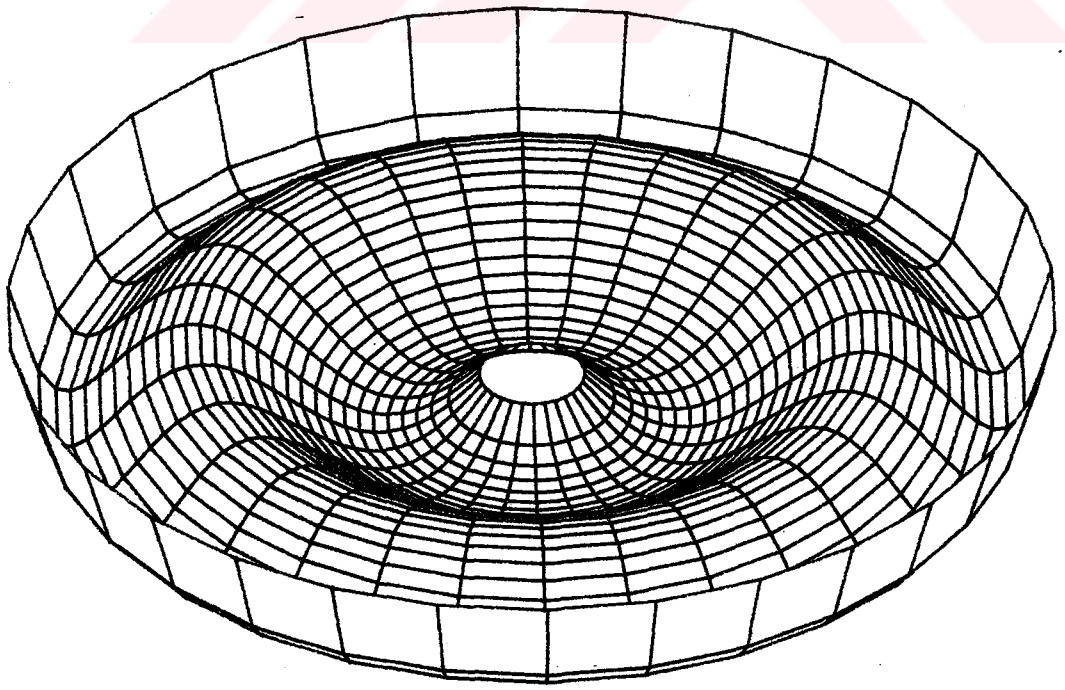

Figure 2.18 : Mode shape corresponding to 0 nodal diameter and 4 nodal circle

$a = 0.2m$
$b = 2.0m$
$\Omega = 10rps$
$k = 1Nt/m$
$m = 1kg/m^2$
$\nu = 0.3$

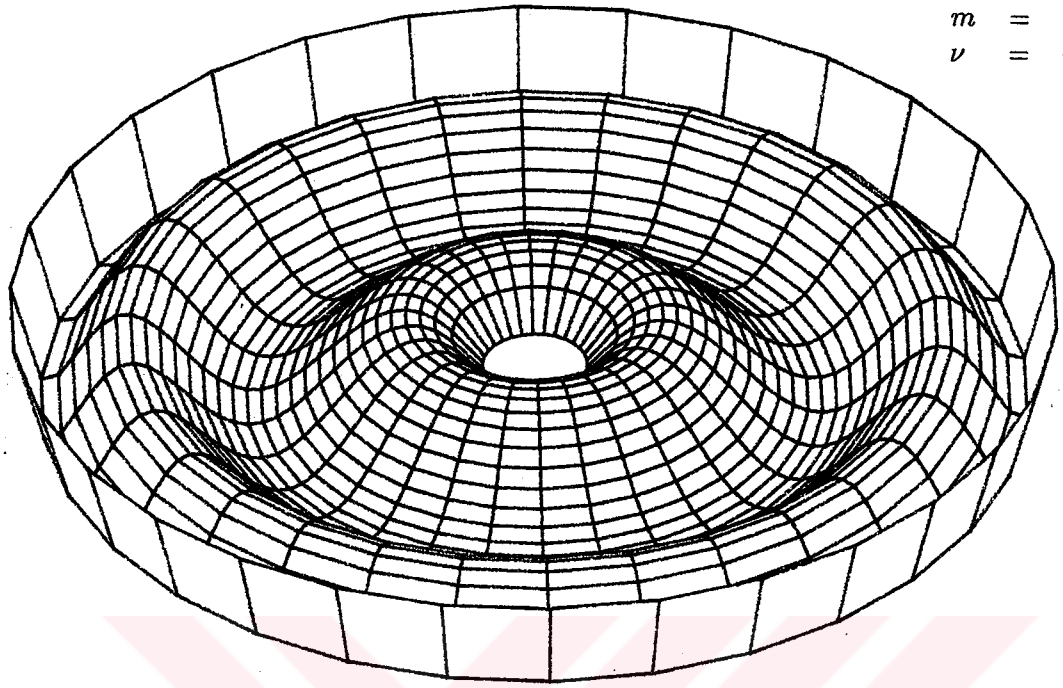

Figure 2.19 : Mode shape corresponding to 0 nodal diameter and 5 nodal circle

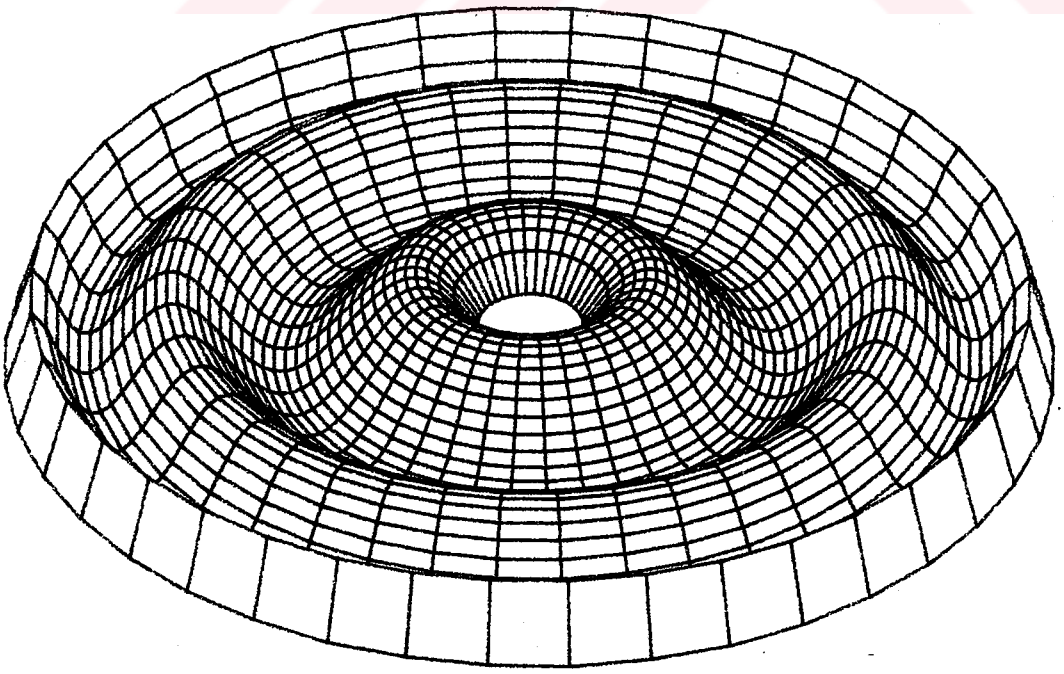

Figure 2.20 : Mode shape corresponding to 0 nodal diameter and 6 nodal circle

$a = 0.2m$
$b = 2.0m$
$\Omega = 10rps$
$k = 1Nt/m$
$m = 1kg/m^2$
$\nu = 0.3$

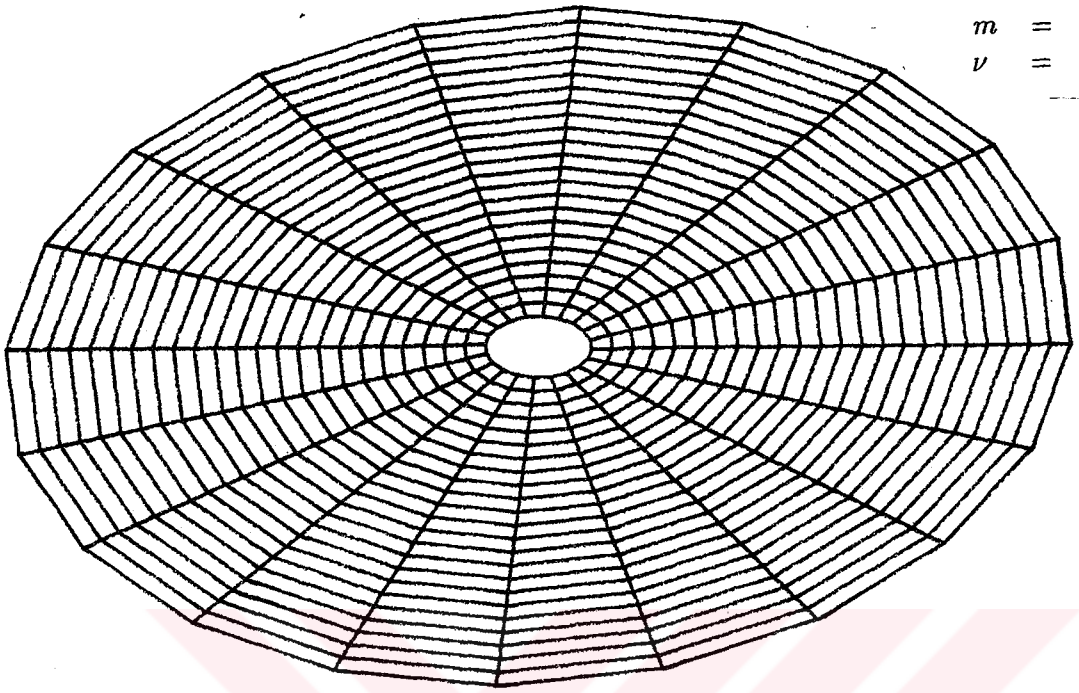

Figure 2.21 : Mode shape corresponding to 1 nodal diameter and 1 nodal circle

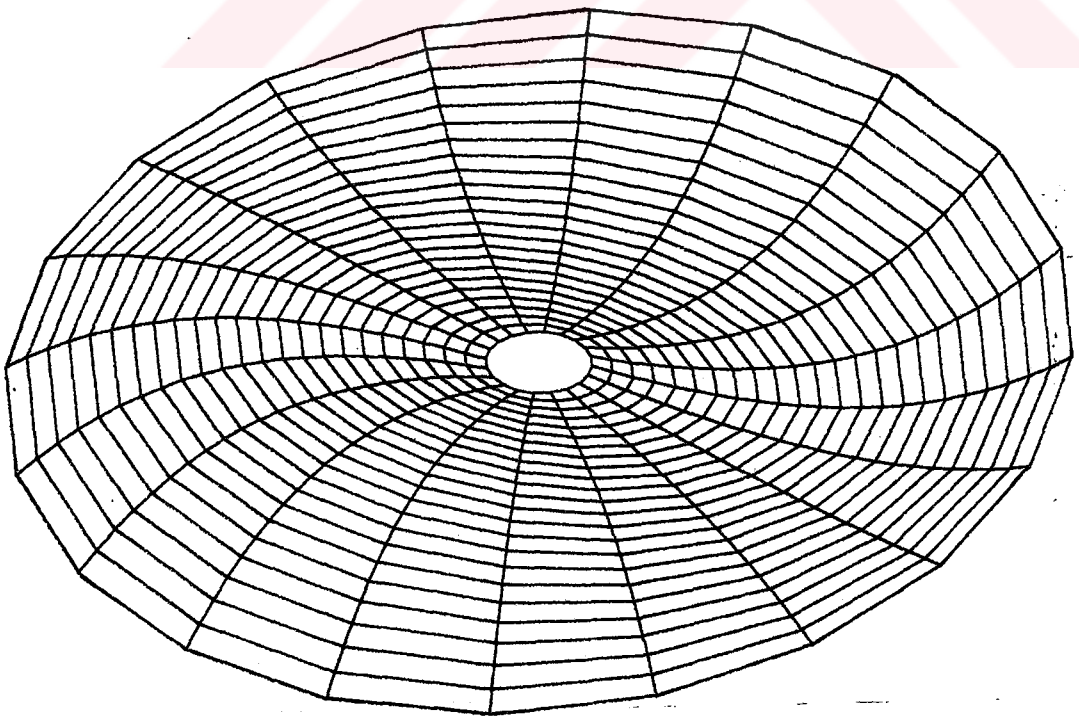

Figure 2.22 : Mode shape corresponding to 1 nodal diameter and 2 nodal circle

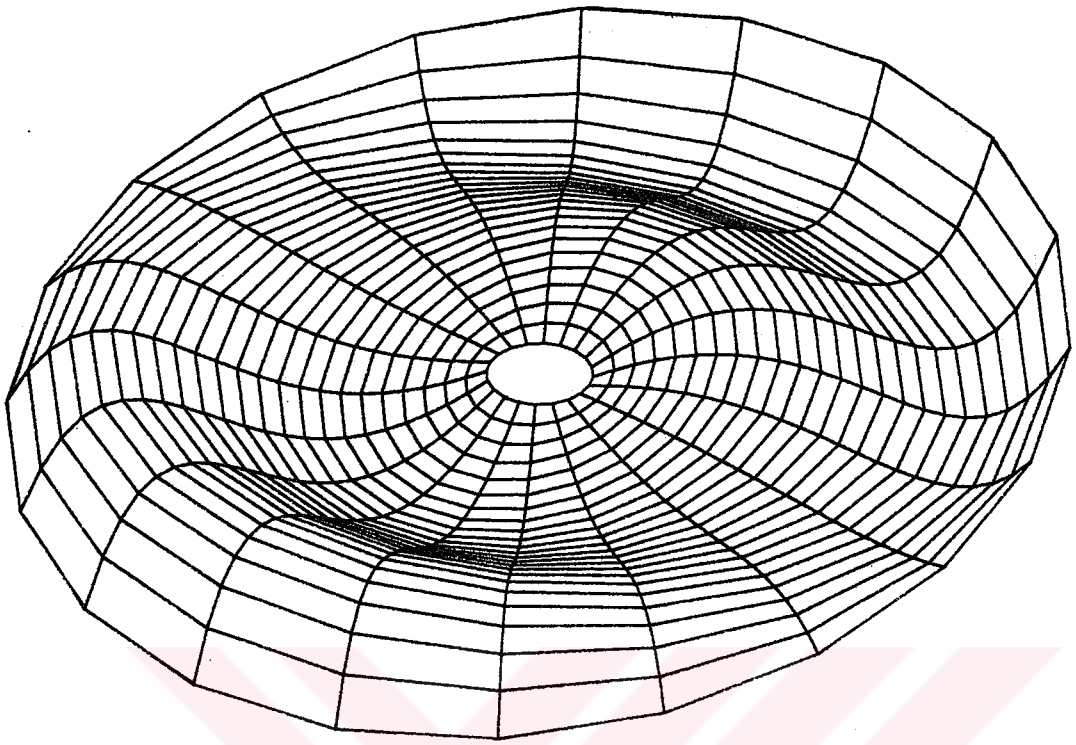

Figure 2.23 : Mode shape corresponding to 1 nodal diameter and 3 nodal circle

$a = 0.2m$
$b = 2.0m$
$\Omega = 10rps$
$k = 1Nt/m$
$m = 1kg/m^2$
$\nu = 0.3$

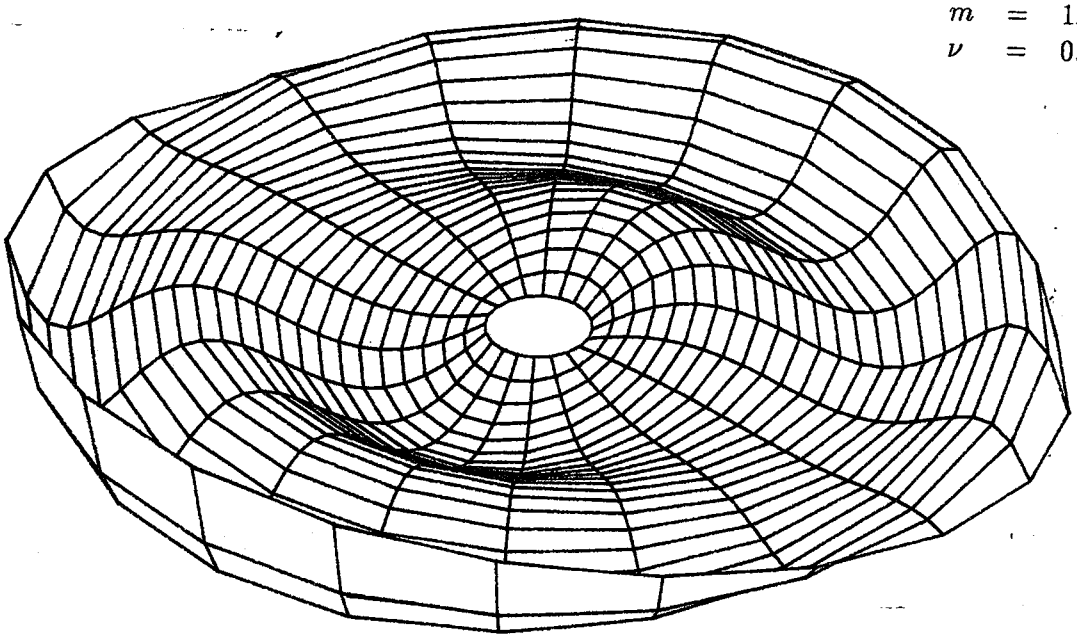

Figure 2.24 : Mode shape corresponding to 1 nodal diameter and 4 nodal circle

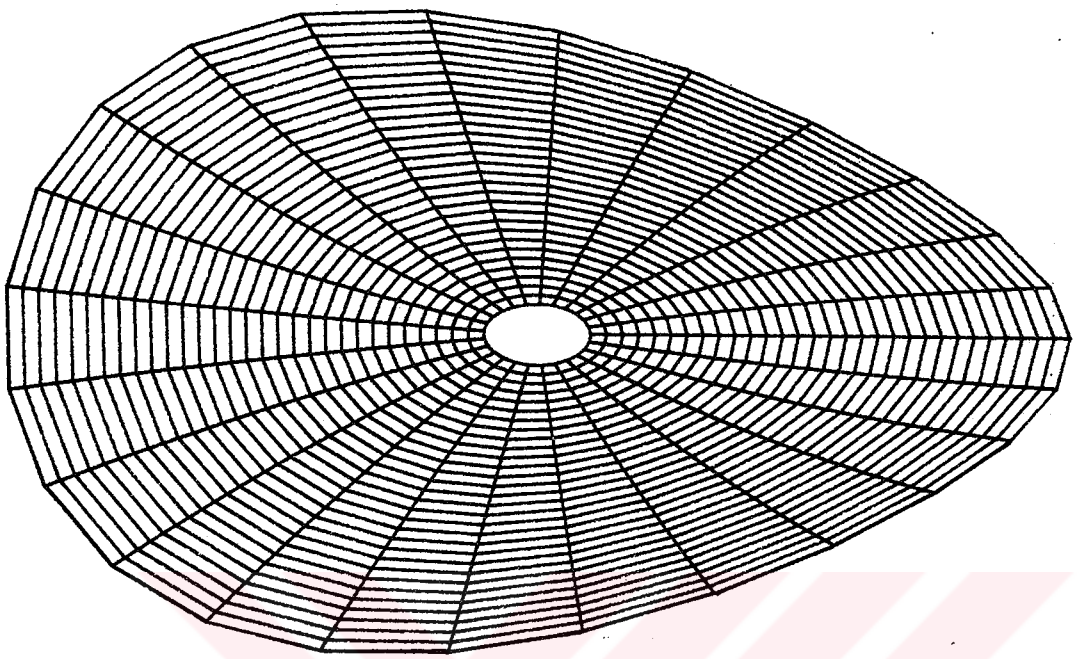

Figure 2.25 : Mode shape corresponding to 2 nodal diameter and 1 nodal circle

$$
\begin{aligned}
a &= 0.2m \\
b &= 2.0m \\
\Omega &= 10rps \\
k &= 1Nt/m \\
m &= 1kg/m^2 \\
\nu &= 0.3
\end{aligned}
$$

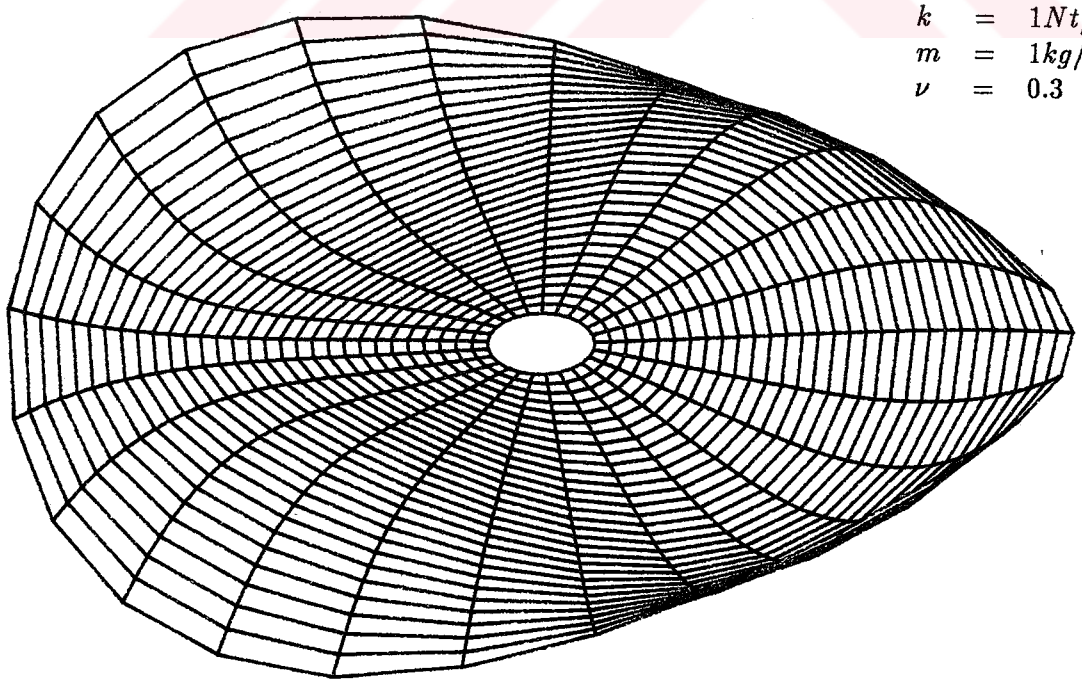

Figure 2.26 : Mode shape corresponding to 2 nodal diameter and 2 nodal circle

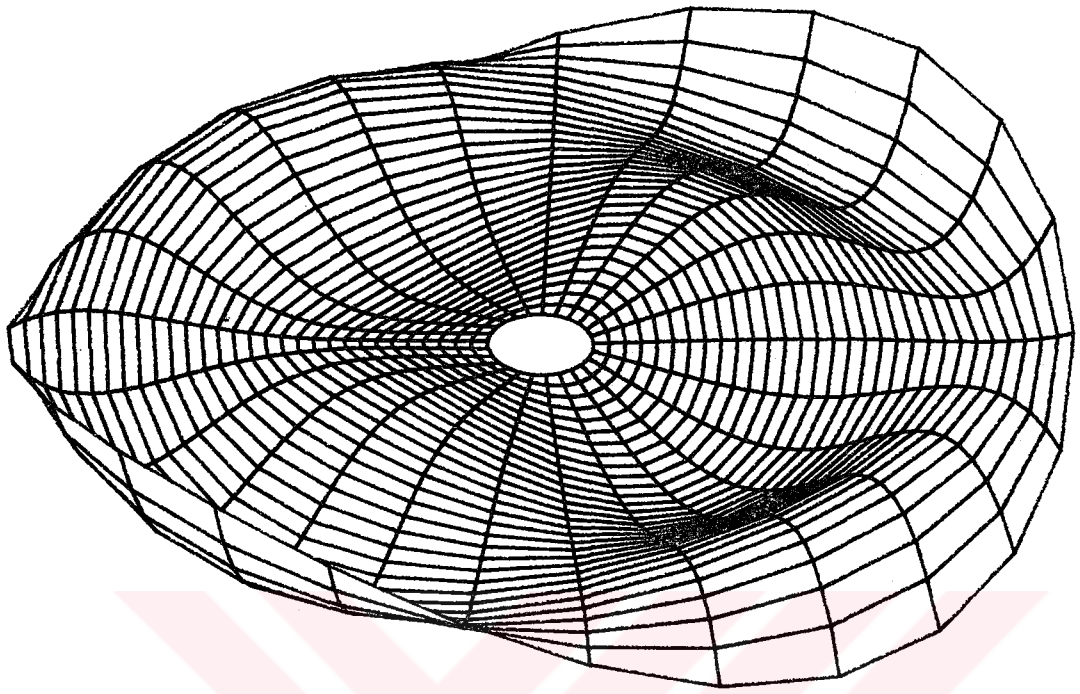

Figure 2.27 : Mode shape corresponding to 2 nodal diameter and 3 nodal circle

$a = 0.2m$
$b = 2.0m$
$\Omega = 10rps$
$k = 1Nt/m$
$m = 1kg/m^2$
$\nu = 0.3$

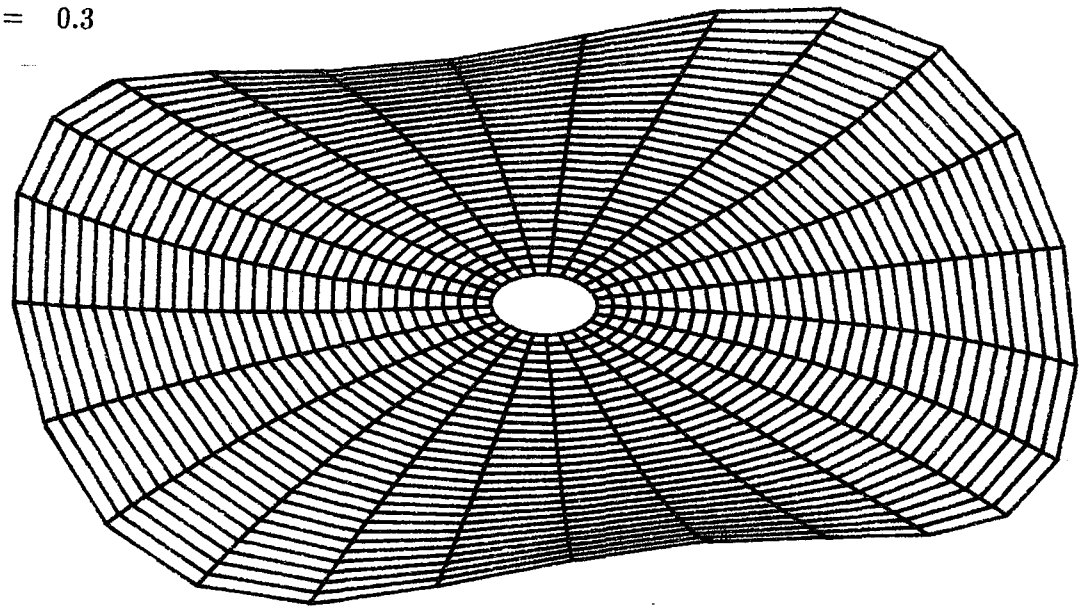

Figure 2.28 : Mode shape corresponding to 3 nodal diameter and 1 nodal circle

$a = 0.2m$
$b = 2.0m$
$\Omega = 10rps$
$k = 1Nt/m$
$m = 1kg/m^2$
$\nu = 0.3$

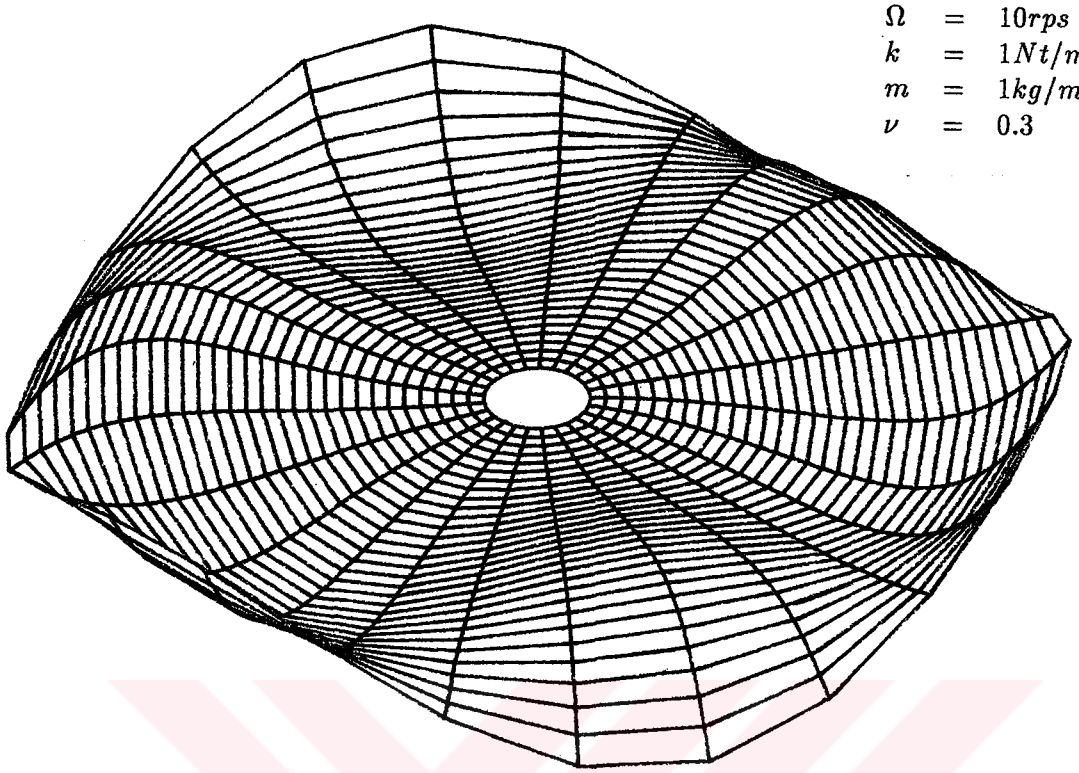

Figure 2.29 : Mode shape corresponding to 3 nodal diameter and 2 nodal circle

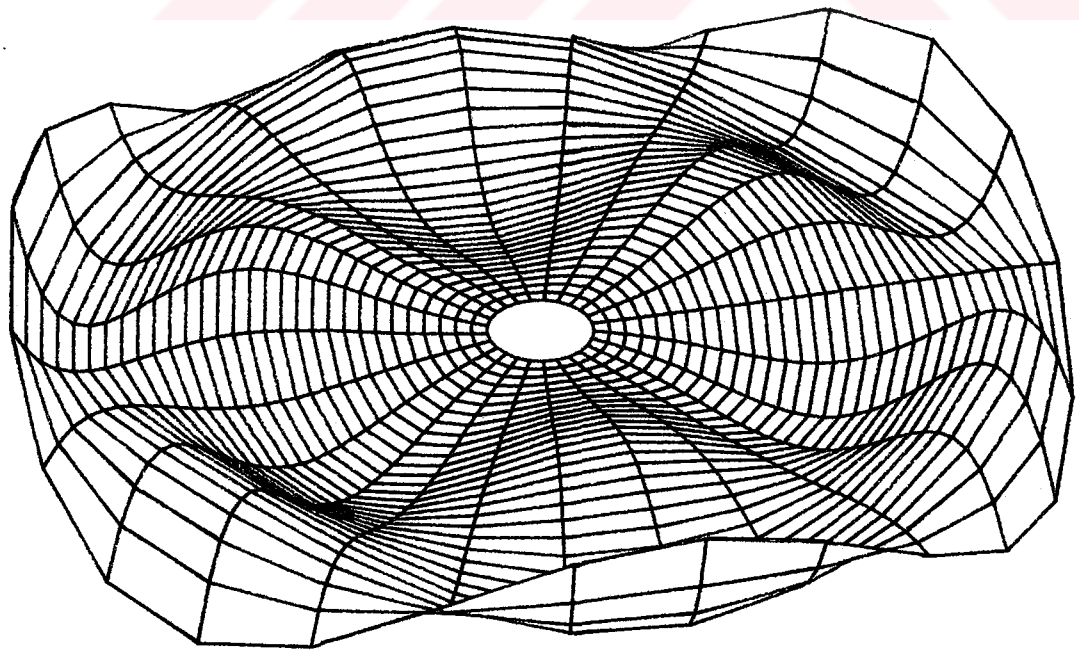

Figure 2.30 : Mode shape corresponding to 3 nodal diameter and 3 nodal circle

$a = 0.2m$
$b = 2.0m$
$\Omega = 10rps$
$k = 1Nt/m$
$m = 1kg/m^2$
$\nu = 0.3$

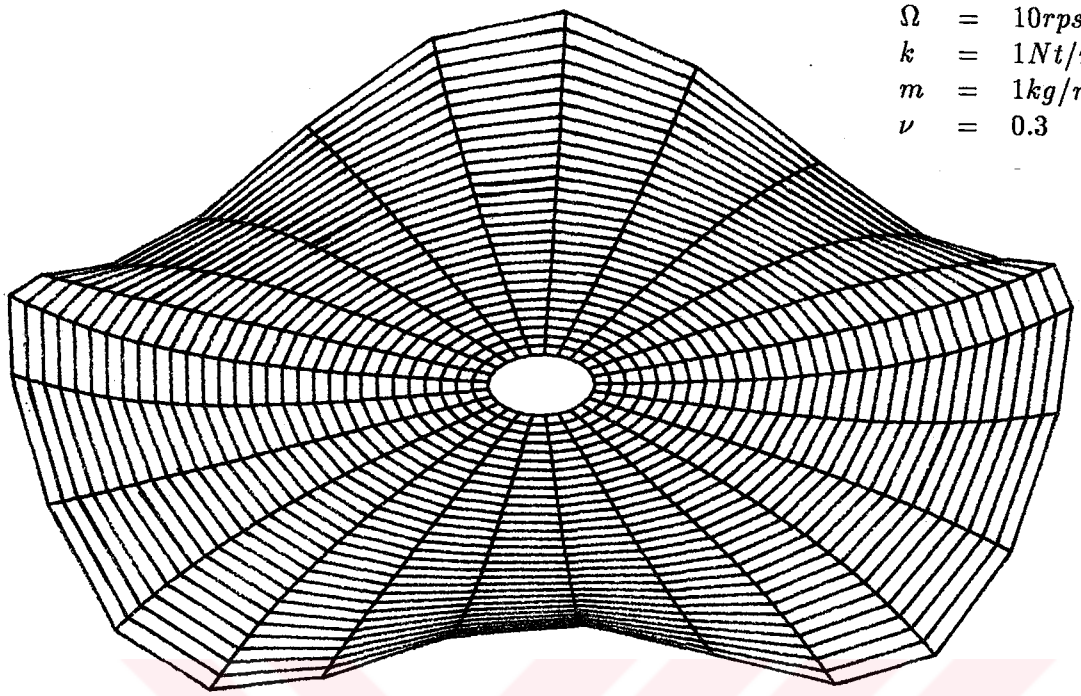

Figure 2.31 : Mode shape corresponding to 4 nodal diameter and 1 nodal circle

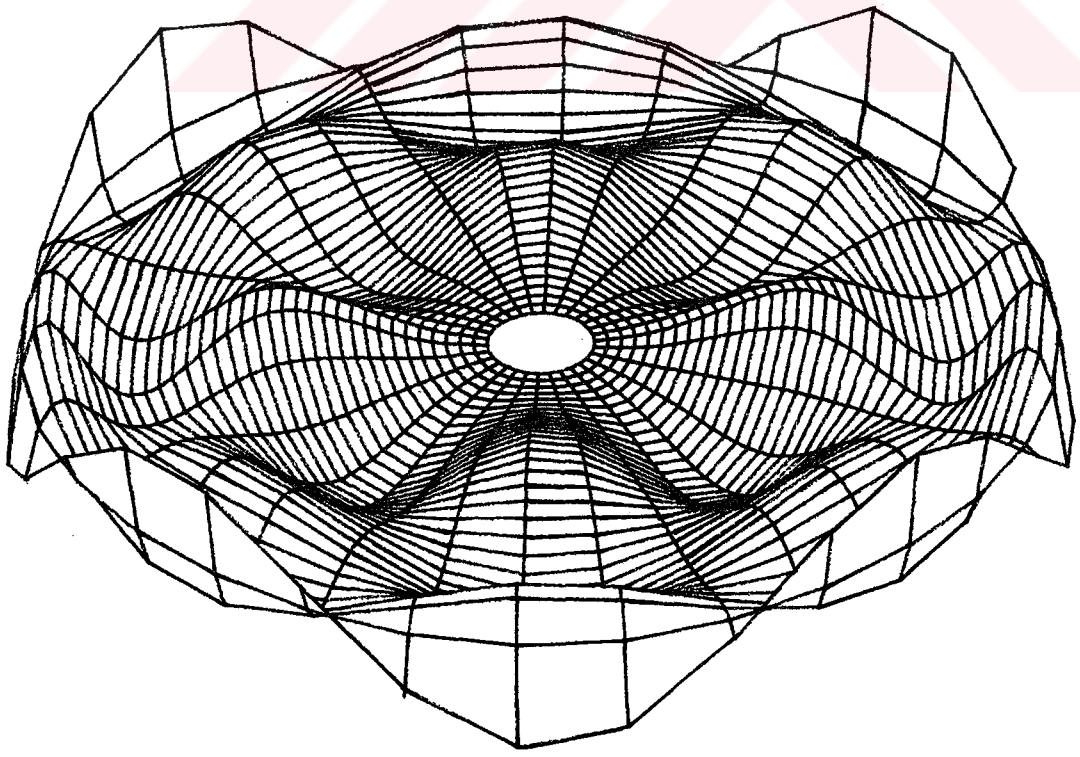

Figure 2.32 : Mode shape corresponding to 4 nodal diameter and 4 nodal circle

$a = 0.2m$
$b = 2.0m$
$\Omega = 10rps$
$k = 1Nt/m$
$m = 1kg/m^2$
$\nu = 0.3$

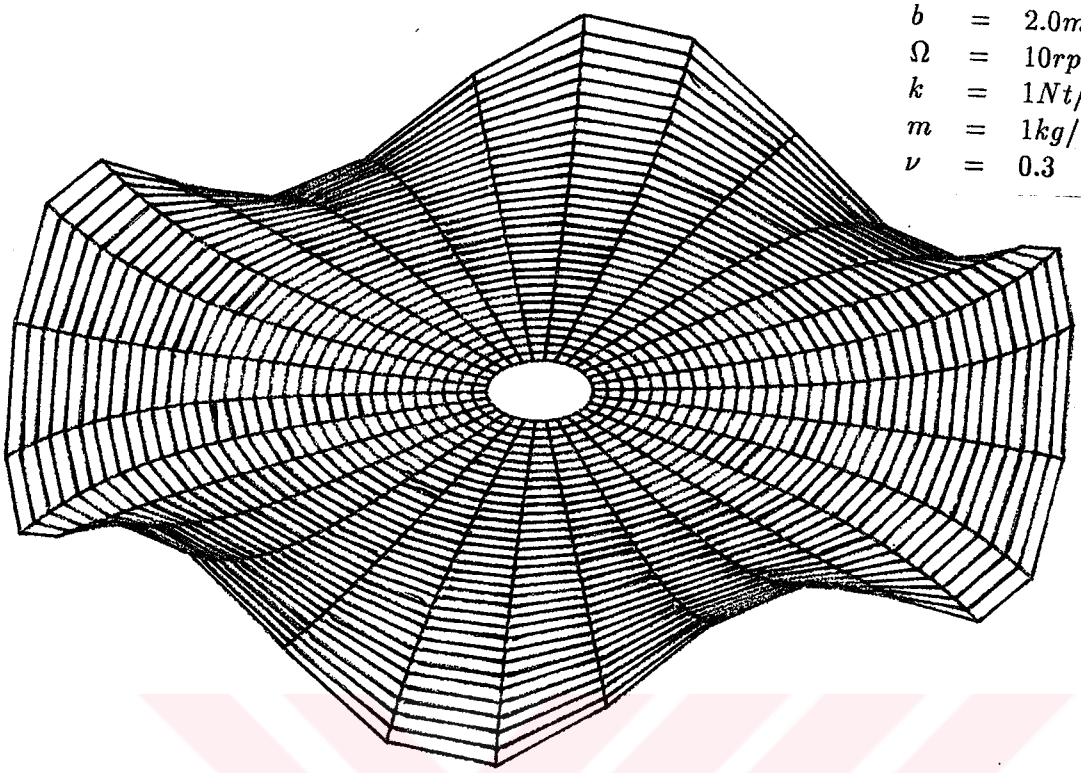

Figure 2.33 : Mode shape corresponding to 5 nodal diameter and 1 nodal circle

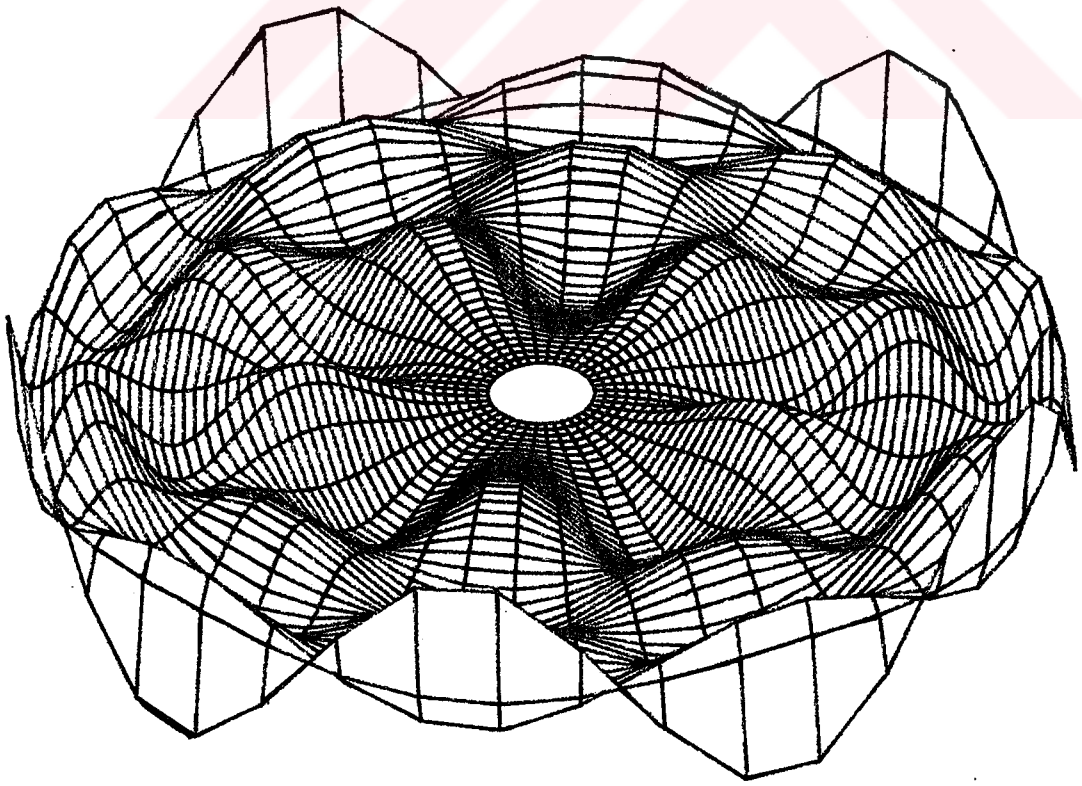

Figure 2.34 : Mode shape corresponding to 5 nodal diameter and 5 nodal circle

CHAPTER 3

RESPONSE OF A CIRCULAR MEMBRANE

3.1 General Formulation

Consider a continuous system described by the partial differential equation

$$L[w(P,t)] + M(P)\frac{\partial^2 w(P,t)}{\partial t^2} = f(P,t) + F_j(t)\delta(P - P_j) \tag{3.1}$$

over domain D. L is a linear homogeneous self-adjoint differential operator. The operator L contains the information concerning the stiffness distribution and $M(P)$ is the mass distribution of the system. The excitation consists of the distributed force $f(P,t)$ and the concentrated forces of amplitude $F_j(t)$ and acting at points $P = P_j$. The symbol $\delta(P - P_j)$ indicates a spatial Dirac's delta function defined by

$$\delta(P - P_j) = 0, \qquad P \neq P_j$$

$$\int_D \delta(P - P_j)dD(P) = 1 \tag{3.2}$$

At every point of the boundary there are p boundary conditions of the type

$$B_i[w(P,t)] = 0, \qquad i = 1, 2, \cdots, p \tag{3.3}$$

where B_i are linear homogeneous differential operators.

The normal modes analysis calls for the solution of the special eigenvalue problem consisting of the differential equation

$$L[w] = \lambda M[w] = \omega^2 M[w] \tag{3.4}$$

The solution of the special eigenvalue problem consists of an infinite set of eigenfunctions $w_r(P)$ with corresponding natural frequencies ω_r.

The eigenfunctions are orthogonal, and if they are normalized such that

$$\int_D M(P) w_r(P) w_s(P) dD(P) = \delta_{rs} \tag{3.5.a}$$

$$\int_D w_r(P) L[w_s(P)] dD(P) = \omega_r^2 \delta_{rs} \tag{3.5.b}$$

Using the expansion theorem we write the solution of the equation (3.1) as a superposition of the normal modes $w_r(P)$ multiplying corresponding time-dependent generalized coordinates $\eta_r(t)$. Hence

$$w(P,t) = \sum_{r=1}^{\infty} w_r(P) \eta_r(t) \tag{3.6}$$

Inserting the equation (3.6) to the equation (3.1), we obtain

$$L[\sum_{r=1}^{\infty} w_r(P)\eta_r(t)] + M(P)\frac{\partial^2}{\partial t^2}\sum_{r=1}^{\infty} w_r(P)\eta_r(t) = f(P,t) + F_j(t)\delta(P - P_j) \tag{3.7}$$

Rearrange the equation (3.7)

$$\sum_{r=1}^{\infty} \eta_r(t) L[w_r(P)] + \sum_{r=1}^{\infty} \ddot{\eta}_r(t) M(P) w_r(P) = f(P,t) + F_j(t)\delta(P - P_j) \tag{3.8}$$

In order to be able to use orthogonality conditios multiply the equation (3.8) by $w_s(P)$ and integrate over domain D

$$\sum_{r=1}^{\infty} \eta_r(t) \int_D w_s(P) L[w_r(P)] dD(P) + \sum_{r=1}^{\infty} \ddot{\eta}_r(t) \int_D w_s(P) M(P) w_r(P) dD(P) =$$

$$\int_D w_s(P)[f(P,t) + F_j(P,t)\delta(P - P_j)] dD(P) \tag{3.9}$$

Assume that we have l number of concentrated load and recalling the defition of the delta function we can write

$$N_r(t) = \int_D w_r(P) f(P,t) dD(P) + \sum_{j=1}^{l} w_r(P_j) F_j(t) \tag{3.10}$$

where $N_r(t)$ denotes a generalized force associated with the generalized coordinate $\eta_r(t)$.

In view of the equations (3.5) and (3.10), the equation (3.9) becomes

$$\ddot{\eta}_r(t) + \omega_r^2 \eta_r(t) = N_r(t), \qquad r = 1, 2, \cdots \tag{3.11}$$

The solution of the equation (3.11) may be obtained by means of the Laplace transform method. Transforming both sides of the equation (3.11)

$$s^2 \bar{\eta}_r(s) - s\eta_r(0) - \dot{\eta}_r(0) + \omega^2 \bar{\eta}_r(s) = \bar{N}_r(s) \tag{3.12}$$

where $\bar{\eta}_r(s)$ and $\bar{N}_r(s)$ are the Laplace transforms of $\eta_r(t)$ and $N_r(t)$, respectively, and $\eta_r(0)$ and $\dot{\eta}_r(0)$ are the initial values associated with the generalized coordinate $\eta_r(t)$. The subsidiary equation is

$$\bar{\eta}_r(s) = \frac{\bar{N}_r(s)}{s^2 + \omega_r^2} + \frac{s}{s^2 + \omega_r^2}\eta_r(0) + \frac{1}{s^2 + \omega_r^2}\dot{\eta}_r(0) \tag{3.13}$$

The equation (3.13) can be inverted by using Borel's theorem

$$\eta_r(t) = \frac{1}{\omega_r}\int_0^t N_r(\tau) \sin\omega_r(t-\tau) d\tau + \eta_r(0)\cos\omega_r(t) +$$

$$\dot{\eta}_r(0)\frac{\sin\omega_r t}{\omega_r}, \qquad r = 1, 2, \cdots \tag{3.14}$$

The integral on the equation (3.14) is known as the convolution integral. The initial generalized displacement $\eta_r(0)$ and initial generalized velocity $\dot{\eta}_r(0)$ are obtained from the expressions

$$\eta_r(0) = \int_D M(P) w_r(P) w(P,0) dD(P)$$

$$\bar{\eta}_r(0) = \int_D M(P) w_r(P) \dot{w}(P,0) dD(P), \qquad r = 1, 2, 3, \cdots \tag{3.15}$$

3.2 Undamped System Response

3.2.1 General Considerations

The excitation can be divided into forcing functions, initial displacements and velocities, and moving supports. The vibration resulting from the action of forcing functions upon a system is known as forced vibration, and the one resulting from initial conditions is called free vibration. Moving supports result in forcing functions in the form of inertia forces and elastic forces and, as such, they lead to forced vibration problems (Ref. [15]).

For the most part the problems of obtaining the response of a continuous system consist of a partial differential equation that the function describing the system response must satisfy throughout a given domain and, in addition, the function must also satisfy associated boundary conditions at every point on the boundaries of the domain. Such problems are called boundary-value problems, and there are various approaches to the solution of such problems. In some cases it might be possible to obtain a solution by means of an integral transformation such as the Laplace or Fourier transformations. In other cases one may be able to assume a solution in the form of an infinite series. The latter approach is modal analysis applied to continuous systems and leads to an infinite set of uncoupled ordinary differential equations. This approach is possible if the separation of variables method can be used to obtain an eigenvalue problem and, one is able to solve the eigenvalue problem. When it is not possible to obtain an exact solution of the eigenvalue problem, one may be content with an appropriate solution, in which case one can still use modal analysis. Approximate methods look upon a continuous system as a finite-degree-of-freedom system and the formulation leads to a set of coupled ordinary differential equations. To obtain an approximate solution of a continuous system by modal analysis it is necessary to solve the eigenvalue problem of a finite-degree-of-freedom system which consists

of symmetric matrices.

3.2.2 Circular Membrane With Moving Supports

Consider a circular membrane with the same properties stated at chapter 2. Let us consider the case in which the supports of a system undergo a known translational motion $u_0(t)$. The absolute displacement of any point can be written $u_0(t)+u(P,t)$, where $u_0(t)$ can be regarded as a rigid-body translation and $u(P,t)$ as an elastic deformation measured relative to the rigid-body motion. If there are no external forces applied, the equation (3.1) can be written.

$$L[u_0(t)+u(r,\theta,t)]+M(P)\frac{\partial^2}{\partial t^2}[u_0(t)+u(r,\theta,t)]=0 \tag{3.16}$$

where L is a differential operator defined previously. But L is such that

$$L[u_0(t)]=A_l(P)u_0(t) \tag{3.17}$$

where $A_l(P)$ is a function of the spatial coordinates, so the equation (3.16) can be written

$$L[u(P,t)]+M(P)\frac{\partial^2 u(P,t)}{\partial t^2}=-M(P)\frac{\partial^2 u_0(t)}{\partial t^2}-A_l(P)u_0(t) \tag{3.18}$$

$$f(P,t)=-M(P) \tag{3.19}$$

where f(P,t) is a known function of time and space. The first term can be identified as a distributed inertia force and the second one as a distributed restoring force.

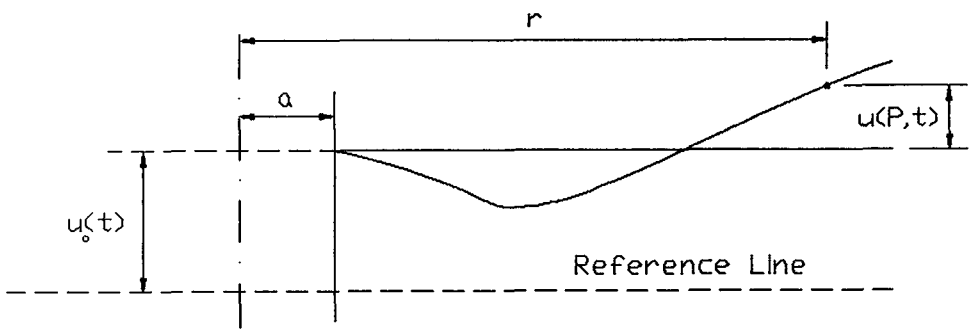

Figure 3.1 : Absolute displacement of any point on the membrane.

The solution of the equation (3.18) can be obtained by following the procedure outlined in Section 3.1.

3.2.3 Response To Harmonic Excitation

In this section, the circular membrane is analyzed in the condition that its boundary at $r = a$ is subjected to translational harmonic motion in the form of $A\sin\omega t$. Therefore $u_0(t)$ in Fig. 3.1 can be written

$$u_0(t) = A\sin\omega t \tag{3.20}$$

Under these circumstances the equation (3.18) can be written

$$L[u(r,\theta,t)] + M(P)\frac{\partial^2}{\partial t^2}[u(r,\theta,t)] = -L[u_0(t)] - M(P)\frac{\partial^2}{\partial t^2}[u_0(t)] \tag{3.21}$$

where

$$L[u_0(t)] = -kA\sin\omega t \tag{3.22}$$

$$M(P)\frac{\partial^2}{\partial t^2}[u_0(t)] = mA\omega^2\sin\omega t \tag{3.23}$$

Introducing the equations (3.22) and (3.23) into the equation (3.21)

$$L[u(r,\theta,t)] + M\frac{\partial^2}{\partial t^2}[u(r,\theta,t)] = A(k - m\omega^2)\sin\omega t \tag{3.24}$$

Right side of the equation (3.24) is only function of time t. Let us define

$$F(t) = A(k - m\omega^2)\sin\omega t \tag{3.25}$$

Next step is coordinate transformation

$$u(r,\theta,t) = \sum_{k=1}^{\infty}\kappa_k(r,\theta)\eta_k(t) \tag{3.26}$$

where $\kappa_k(r,\theta)$ was calculated by means of free vibration analysis in Chapter 1 and $\eta_k(t)$ is calculated by modal analysis. Inserting the equation (3.26) into the equation (3.24), and using orthogonality conditions (3.5), and after some mathematical manipulations we obtain

$$\ddot{\eta}_k(t) + \omega_k^2\eta_k(t) = N_k(t), \qquad k = 1,2,\cdots \tag{3.27}$$

where

$$N_k(t) = \int_D \kappa_k(r,\theta) F(t) dr d\theta \tag{3.28}$$

The solution of the equation (3.27) may be obtained by means of the Laplace transform method.

$$\eta_k(t) = \frac{1}{\omega_k} \int_0^t N_k(\tau) \sin \omega_k (t-\tau) d\tau + \eta_k(0) \cos \omega_k(t) +$$

$$\dot{\eta}_k(0) \frac{\sin \omega_k t}{\omega_k}, \qquad k = 1, 2, \cdots \tag{3.29}$$

where $\eta_k(0)$ is the initial generalized displacement and $\dot{\eta}_k(0)$ is the initial generalized velocity, and these are obtained from the equation (3.15). In our case

$$u(r,\theta,0) = 0 \tag{3.30.a}$$

$$\dot{u}(r,\theta,0) = 0 \tag{3.30.b}$$

Therefore

$$\eta_k(0) = 0 \tag{3.31.a}$$

$$\dot{\eta}_k(0) = 0 \tag{3.31.b}$$

3.3 Numerical Results

In this analysis the same admissible function being taken in the previous chapter is used. Since the excitation frequency is near to the first and the second frequency of the system, in the shapes, as it is seen, the effect of the first and second mode shapes is more dominant. The effect of the other mode shapes is not obvious. The first and second frequency of the system are $13.89Hz$, $46.56Hz$ respectively, and the excitation frequency is $20.00Hz$. The results are presented by means of the shapes in the next pages.

$a = 0.2m$
$b = 2.0m$
$\Omega = 10rps$
$k = 1Nt/m$
$m = 1kg/m^2$
$\nu = 0.3$

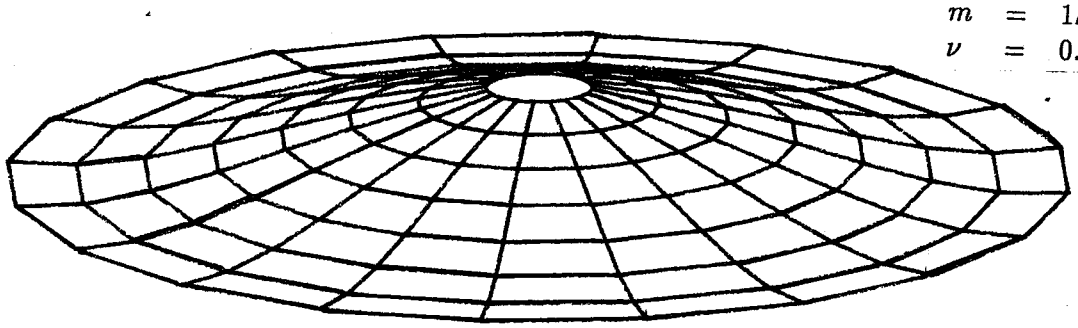

Figure 3.2 : Disk geometry at $t = 0.25$ sec. due to excitation

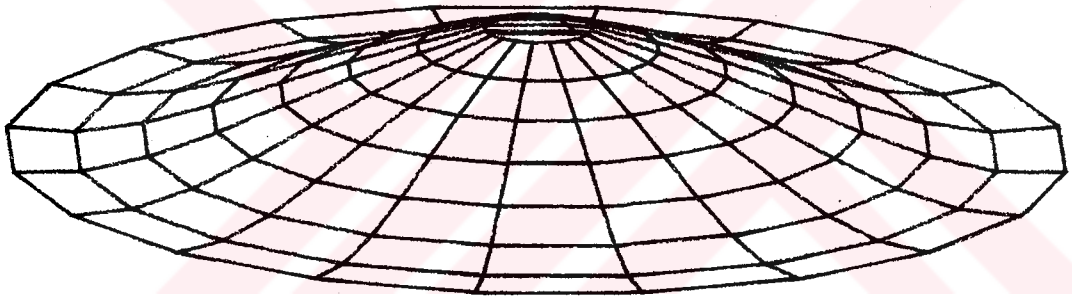

Figure 3.3 : Disk geometry at $t = 0.40$ sec. due to excitation

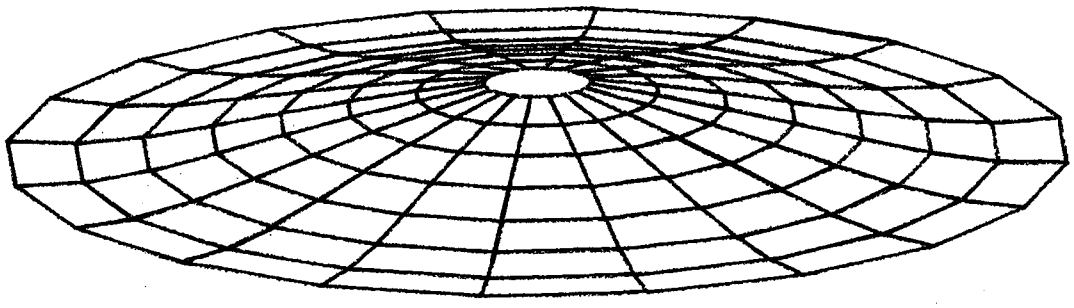

Figure 3.4 : Disk geometry at $t = 0.60$ sec. due to excitation

$a = 0.2m$
$b = 2.0m$
$\Omega = 10rps$
$k = 1Nt/m$
$m = 1kg/m^2$
$\nu = 0.3$

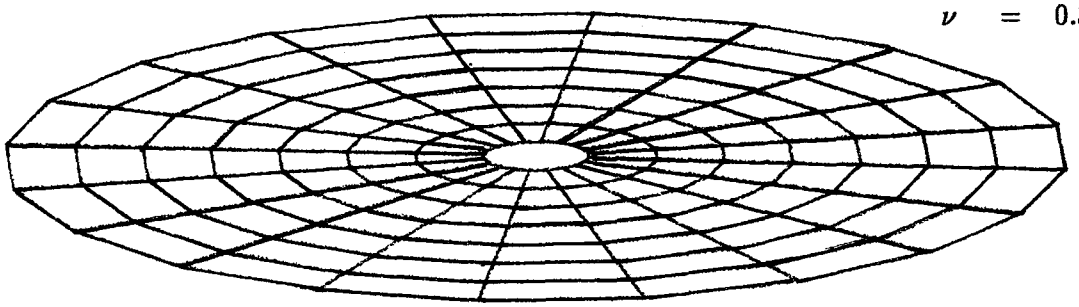

Figure 3.5 : Disk geometry at $t = 0.90$ sec. due to excitation

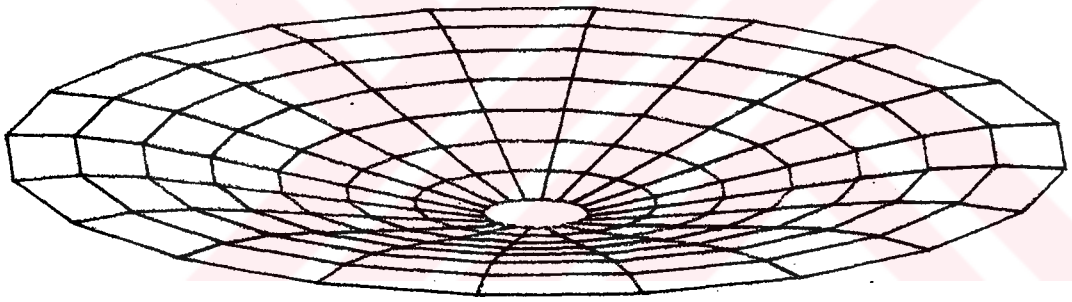

Figure 3.6 : Disk geometry at $t = 1.00$ sec. due to excitation

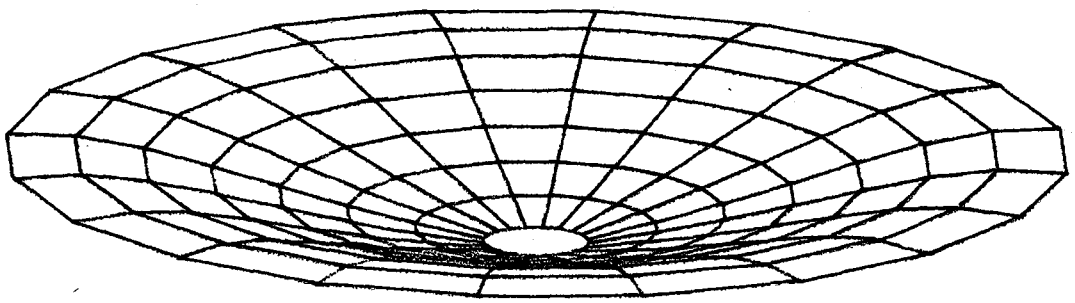

Figure 3.7 : Disk geometry at $t = 1.30$ sec. due to excitation

CHAPTER 4

A Different Approach with Applied Structure Software

4.1 General Purpose Software

Applied Structure software is a product of Rasna Corporation, which was founded in November 1987 by physicists and mechanical engineers from IBM's Almaden Research Center. The program allows engineers to construct computer models of structures or components, apply loads, and study stress effects without having to build the object or destroy it in testing.

The software is used in a wide variety of disciplines, ranging from the aerospace and automotive industries to civil construction. The program has been used to analyze such everyday items as aluminum cans, paper clip, and hair dryer, as well as for designing bridges, and machinery crank. Applied Structure is used to solve many types of analyses, including structural, mechanical, thermal analyses. Also, the results can be expressed in a variety of ways, as displacements, stresses, and strains in color-coded graphic displays or in text.

Applied Structure is used for static, dynamic, and vibrational analyses and includes preprocessing, solution, and postprocessing. These analses can be

done in one, two, or three dimensions. With these capabilities, large, complex systems can be modeled and analyzed. Once the model is built, analysts can specify boundary conditions applicable to the model which can be displayed graphically. Solution output can be displayed graphically.

Finite Element Analysis is the most commonly used numerical method for the structural problems. The most commercial softwares use the h-version of FEA. An alternative method of the h-version of FEA is called the p-version. In p-extension the finite element mesh is usually much simpler than in h-extension and the time required for data preparation is substantially less. Therefore, the overall cost of analysis is substantially less. Importantly, p-extension produces a strongly sequence of solutions at a small marginal cost and in a small amount of additional time.

Sequences of discretization can be constructed in various ways: by mesh refinement, increasing the degree of the standard polnomial space, or any combination of these. For reasons of implementation most commonly the mesh is refined, or the degree of the standard polynomial space is increased, or mesh refinement is combined with increase of the polynomial degrees. These approaches are respectively call h-extension, p-extension and hp-extension.

By using p-version Applied Structure can define a model with fewer and larger elements, substantially simplifying modeling for analysis.

4.2 Modeling within Applied Structure and Results

Firstly model geometry is created by using the drawing and editing commands. Secondly model elements are built on geometry and material properties are specified. In this problem four planar four-sided shells are used to build elements.Then a centrifugal force that acts on the entire model is defined by entering

the angular velocity. Additionaly boundary conditions are defined.

After all above things, the static analysis is performed in order to obtain stress and strain distribution on the model. Since this analysis is simpler than the modal analysis, the model is constructed three-dimensionally (Figure 4 .1). The results are taken in color-coded graphic displays due to allowing the quick interpretation.

But in order to be able to obtain mode shapes, due to not enough capacity of the computer on which the software runs, two-dimensional modal analysis can be specified. In spite of performing two-dimensional analysis, only first five mode shapes can be found.

The outputs of Applied Structure are presented in the following pages.

$a = 0.2m$
$b = 2.0m$
$\Omega = 10rps$

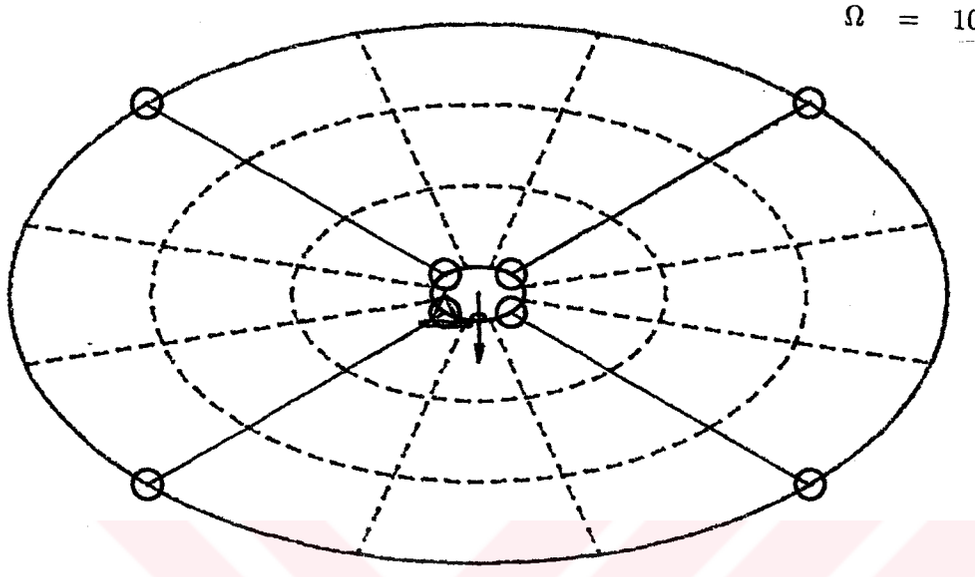

Figure 4.1 : 3D model for stress-strain analysis

$a = 0.2m$
$b = 2.0m$
$\Omega = 10rps$

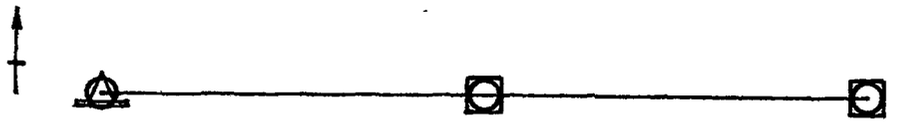

Figure 4.2 : 2D model for modal analysis

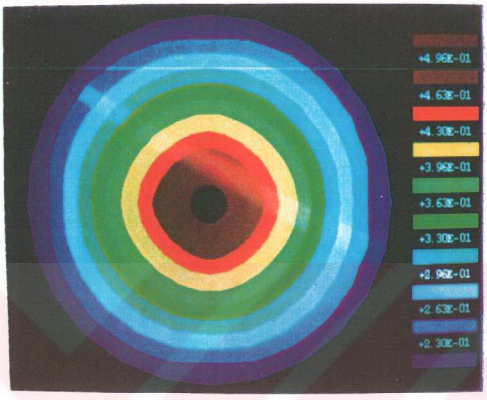

Figure 4.3 : von Mises stress analysis results

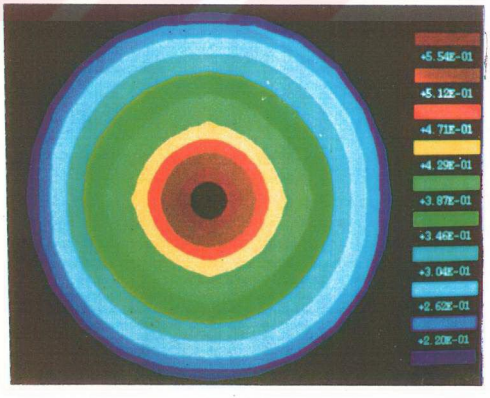

Figure 4.4 : Maximum principles stress analysis results

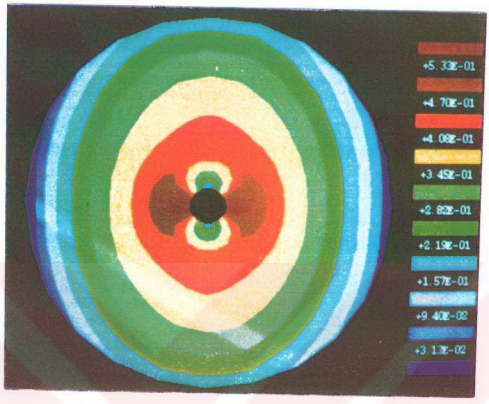

Figure 4.5 : σ_{xx} stress analysis results

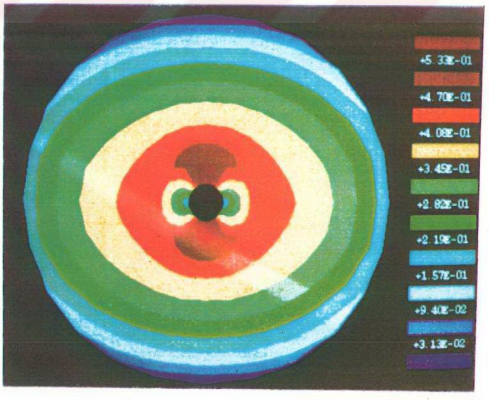

Figure 4.6 : σ_{yy} stress analysis results

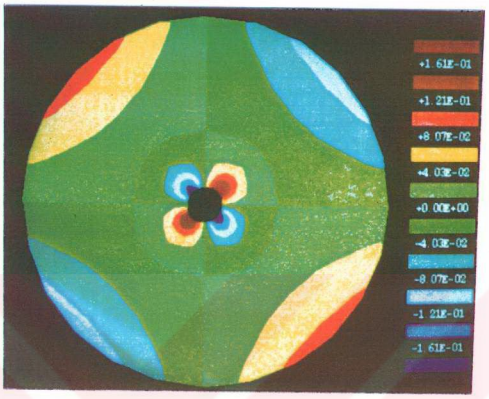

Figure 4.7 : σ_{xy} stress analysis results

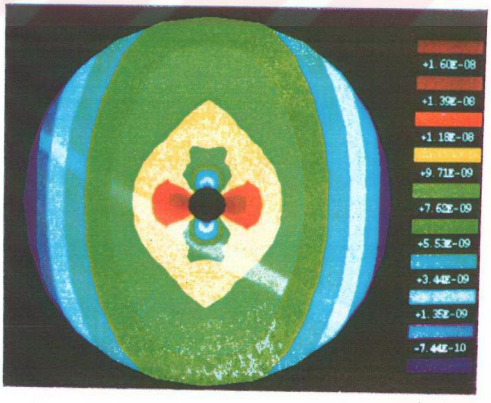

Figure 4.8 : u_{xx} strain analysis results

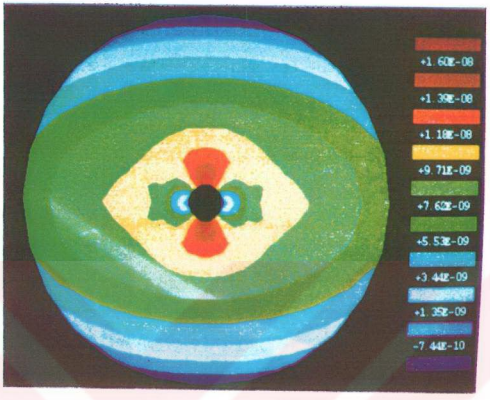

Figure 4.9 : u_{yy} strain analysis results

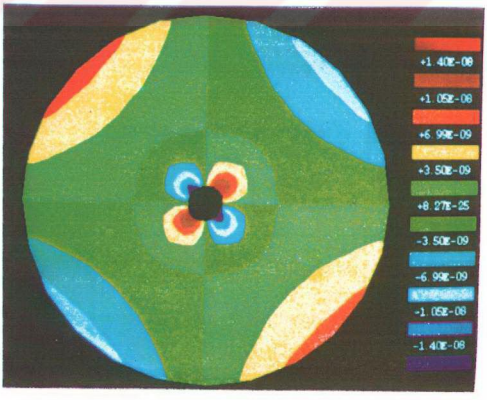

Figure 4.10 : u_{xy} strain analysis results

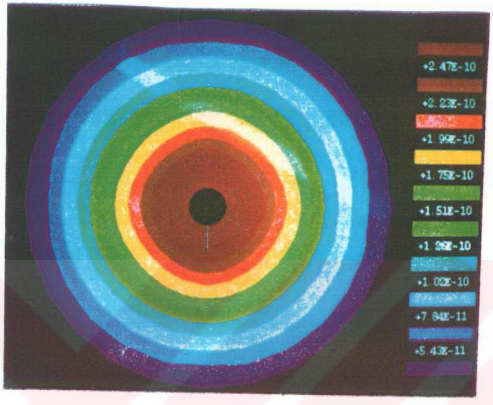

Figure 4.11 : Membrane strain energy analysis results

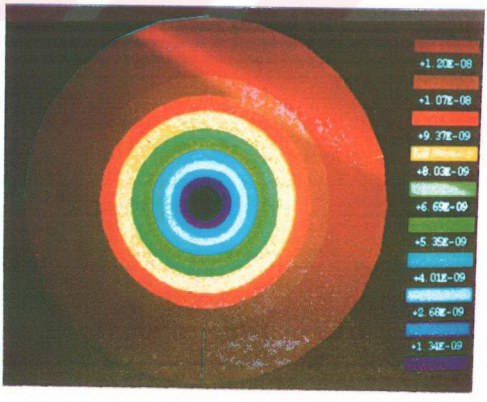

Figure 4.12 : Displacement magnitute analysis results

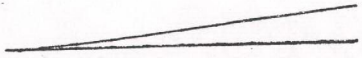

(a)

(b)

(c)

(d)

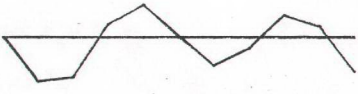

(e)

Figure 4.13 : Modal analysis result showing first five mode shapes
(a) first mode shape, (b) second mode shape,
(c) third mode shape, (d) fourth mode shape,
(e) fifth mode shape

CHAPTER 5

CONCLUSIONS AND DISCUSSIONS

In this thesis a circular membrane with a centrally hole on a circle of radius a on elastic foundation which is taken to be rigidly clamped on a circle of radius a and free at the outer edge is examined. The mode shapes are obtained two-dimensionally and three-dimensionally and the frequencies' variation versus the most important quantities is plotted. Then the membrane is considered to subject the harmonic excitation in the condition that the support is moving translationaly in the form of $A \sin \omega t$. Under these circumstances undamped system response is reached. At any of time disk geometry due to excitation can be found. Finally the problem with the exception of the effect of elastic foundation is modeled in the Applied Structure software. Stress and strain distributions and modal analysis results involving the first five mode shapes are presented.

In order to solve the problem numerically, in the beginning of the analysis the solution is chosen as a sin series. It is important how many terms are taken in the analysis. Of course the results are more accurate with increasing the number of the terms of the series. But the more term causes the more computational time. In the solutions the first fourteen terms are taken.

It can be said that the frequencies are not affected by the variation of the poisson ratio. The variation of the coefficient of the springs representing the elastic foundation causes very little increment in the frequencies and does not effect the mode shapes. But the frequencies are going up obviously with increasing the clamp radius a, and the angular velocity Ω. Because the system is more stiff with increasing the clamp radius and the angular velocity. The reason is that the elastic forces are more dominant than the inertia forces.

In addition the mode shapes finding in Chapter 3 are same as the mode shapes obtaining from the analysis of Applied Structure software. This situation implies that the analyses done are true.

From the results of the modal analysis done in Chapter 3, it can be said that when the frequency of harmonic excitation is equal to the frequencies of the system, displacements on the membrane goes to infinity, that is, resonance occurs. Additionaly if the frequency of the harmonic excitation is near to which frequency of system, membrane's shape due to excitation is the same as mode shape belonging to that frequency.

In this study the vibration within the plane of the membrane is not taken into consideration.

REFERENCES

[1] Benson, R.C. and Bogy, D.B., Deflection of a Very Flexible Spinning Disk Due to a Stationary Transverse Load, Transactions of the ASME, vol. 45, pp 636–642, 1978

[2] Simmonds, J.G., The Transverse Vibrations of a Flat Spinning Membrane, Journal of the Aerospace Sciences, vol. 29, pp 16–18, 1962

[3] Eversman, W., Transverse Vibrations of a Clamped Spinning Membrane, AIAA Journal, vol. 6, pp 1395–1396, 1968

[4] Eversman, W. and Dodson, R.O., Jr., Free Vibration of a Centrally Clamped Spinning Disk, AIAA Journal, vol. 7, pp 2010–2012, 1969

[5] Barasch, S. and Chen, Y., On the Vibration of a Rotating Disk, Journal of Applied Mechanics, vol. 39, pp 1143–1144, 1972

[6] Mote, C.D., Jr., Free Vibration of Initially Stressed Circular Disks, Journal of Engineering for Industry, pp 258–264, 1965

[7] Haigh, R.E. and Murdoch, M.L., Analysis of Centrifugal Stresses in Turbine Wheels, Journal Mechanical Engineering Sciences, vol. 5, pp 66–74, 1963

[8] Seirag, A. and Surana, K.S., Optimum Design of Rotating Disks, Journal of Engineering for Industry, pp 1–10, 1970

[9] Seirag, A. and Surana, K.S., Design of Rotating Disks with Integral Shafts, Journal of Engineering for Industry, pp 805–813, 1971

[10] Pardoen, G.C., Static, Vibration and Buckling Analysis of Axisymmetric Circular Plates Using Finite Elements, Computers and Structures, vol. 3, pp 355–375, 1973

[11] Kirkhope, J. and Wilson, G.J., Vibration and Stress Analysis of Thin Rotating Discs Using Annular Finite Elements, Journal of Sound and Vibration, pp 461–474, 1976

[12] Nigh, G.L. and Olson, M.D., Finite Element Analysis of Rotating Disks, Journal of Sound and Vibration, pp 61–78, 1981

[13] Good, J.K. and Lowery, R.L., The Finite Element Modeling of the Free Vibration of a Read/Write Head Floppy Disk System, Journal of Vibration, Acoustics, Stress, and Reliability in Design, vol. 107, pp 329–333, 1985

[14] Mote, C.D. and Szymani, R., Principal Developments in Thin Circular Saw Vibration and Control Research, Holz als Roh–und Werkstoff, pp 189–196, 1977

[15] Meirovitch, L., Analytical Methods in Vibrations, the Macmillan Company, 1967

CURRICULUM VITAE

Barbaros SOYER was born in Ankara–TURKIYE on August 10, 1967. He graduated from high school in 1984. He obtained his B.Sc. degree from Istanbul Technical University, Department of Aeronautical Engineering, in 1988. Same year he started his M.Sc. education in Middle East Technical University. In 1990, he came to Istanbul Technical University to carry on his M.Sc. studies. He has been employed as an application engineer on the topics related to Computer Aided Design and Engineering by private companies for two years. He is single.